



**NARSIS**

**New Approach to Reactor Safety Improvements**

## **WP2: Fragility assessment of main NPPs critical elements**

### **D2.4 - Methodology to account for ageing mechanisms in the fragility assessment**



This project has received funding from the Euratom research and training programme 2014-2018 under Grant Agreement No. 755439.





## Table of contents

<b>1</b>	<b>Executive Summary .....</b>	<b>8</b>
<b>2</b>	<b>Introduction .....</b>	<b>9</b>
<b>3</b>	<b>Ageing.....</b>	<b>11</b>
3.1	Effects of ageing on the integrity of plant .....	13
3.2	Methodological approach for ageing .....	13
3.3	Referential NPP model.....	15
<b>4</b>	<b>Seismic investigation .....</b>	<b>19</b>
4.1	FE model description.....	19
4.2	Seismic analysis.....	21
4.2.1	<i>Numerical simulations</i> .....	23
4.2.2	<i>Modal Analyses</i> .....	24
4.2.3	<i>Transient Analysis</i> .....	26
4.3	Main conclusions.....	31
<b>5</b>	<b>Aged primary piping analysis .....</b>	<b>32</b>
5.1	Ageing analysis: the pipe thinning .....	33
5.1.1	<i>Analysis of an aged straight pipe</i> .....	34
5.1.2	<i>Straight pipe analysis results</i> .....	35
5.1.3	<i>Analysis of an aged bent pipe</i> .....	39
5.1.4	<i>Bent pipe analysis results</i> .....	42
5.2	Main conclusions.....	46
<b>6</b>	<b>Conclusions .....</b>	<b>48</b>
<b>7</b>	<b>References.....</b>	<b>49</b>

## List of Figures

Figure 1: Generic definition of the time frame known as LTO period.....	9
Figure 2: Integration of component-specific ageing with plant or system level analysis.....	10
Figure 3: Conceptual component safety state .....	11
Figure 4: Systematic approach for ageing [4].....	12
Figure 5: The most important ageing mechanisms and consequences for a NPP item (from [5]).....	13
Figure 6: Approach for determining risk sensitivity to component ageing.....	14
Figure 7: (a) Main SSCs of the generic PWR containment system and (b) vertical cross-sections of the double wall containment structure [mm]. The inner containment diameter is about 46 m .....	16
Figure 8: (a) RPV vertical section with weight data [system unit: ton]; (b) RPV (left) and RPV lower head (right) with main dimensions [mm].....	17
Figure 9: SG vertical section with main dimensions [mm] .....	18
Figure 10 a, b, c: Overview of the geometrical model and FE model of Gen III NPP (a). In (b) the containment system, and in (c) the horizontal and vertical steel reinforcement arrangements are shown.....	22
Figure 11: Detail of the NPP model: arrangement of 4 SGs, bottom and lateral lower supports included, and piping. The term half identifies the symmetric part of the systems .....	23
Figure 12: First modal shape of the outer and inner reactor containment, respectively. In (b) the results of the modal analysis carried out on the overall plant confirming that the 1 <sup>st</sup> “cantilever” mode outer reactor containment is at about 3.6 Hz .....	25
Figure 13 a, b: (a) Horizontal and vertical ATHs calculated at the node 98415, representative of the connection between pipeline and SG4, as an example. (b) Module of the acceleration for ATH50.....	28
Figure 14: Acceleration comparison for ATH50 between aged (blue curve) and unaged (green curve) NPP at the internal containment hemispherical roof wall. ....	29
Figure 15: Example of Von Mises stress comparison for ATH50 between aged (blue curve) and unaged (green curve) NPP at the internal containment hemispherical roof wall. For ageing assessment temperature dependent material properties were taken into account. ....	29
Figure 16: Example of acceleration counter plot for ATH50 input for aged (left) and unaged (right) at t=20s.....	30
Figure 17: Example of displacement counter plot for ATH50 input for aged (left) and unaged (right) at t=20s .....	30
Figure 18: Example of equivalent stress counter plot for ATH50 input for aged (left) and unaged (right) at t=20s	31
Figure 19: Schematic diagram for thinning investigation. In the top right table are summarised some experimental based value of the wearing thinning rate for different primary fluid conditions to take into account for analysis [33].....	32
Figure 20: Schematic cross-section of a straight pipe. The geometry was reproduced exactly in the FE model ..	35
Figure 21 a, b: Equivalent Von Mises stress(a) (at the bottom layer) and the resulting plastic deformation (b) for localised and heterogeneous thickness reduction. The nominal pipe thickness, 30 yr aged, is $t_{nom}=1.55$ cm (Table 6); while the section with localized thinning has $t_{reduced}=0.8$ cm .....	37
Figure 22 a, b, c: Equivalent Von Mises stress (at the bottom layer) for pipe subjected to homogenous thinning (a) and thinning localized along a generatrix (b) and in a part of pipe (c). In these simulations, actual yielding strength is considered.....	38
Figure 23: Equivalent Von Mises stress (at the bottom layer) of pipe subjected to heterogeneous and accelerated thinning-AT- (orange colored).....	39
Figure 24: Cross-section of the bent pipe. Geometrical dimensions are in [m] .....	39
Figure 25: 3D FE model of the bent pipe.....	40

Figure 26: Equivalent Von Mises stress bottom layer – Case 5 ..... 43

Figure 27: Equivalent Von Mises stress bottom layer – Case 5 ..... 43

Figure 28: Total equivalent creep strain – Case 5 ..... 43

Figure 29: Top and bottom equivalent layers of equivalent von Mises stress away from thinning – Case 1 (reference); Case 4; Case 5 ..... 44

Figure 30: Top and bottom layers of equivalent von Mises stress in thinning - Case 1 (reference); Case 4; Case 5 ..... 44

Figure 31: Top and bottom layers of equivalent von Mises stress in thinning - Case 1 (reference); Case 4; Case 5 ..... 45

Figure 32: Top and bottom layers of equivalent von Mises stress in thinning – Case 3 ..... 45

## List of Tables

Table 1: Main ageing mechanisms .....	12
Table 2: Material properties of NPP components .....	18
Table 3: Steel rebars properties .....	20
Table 4: Modal analysis results .....	25
Table 5: Monitoring points location .....	26
Table 6: Residual pipe wall thickness allowing the extension of life .....	35
Table 7: Residual life (Lr) beyond 30 years operation vs structural strength decrease .....	36
Table 8: Thermo-mechanical properties of AISI304 [32] .....	41
Table 9: Residual life (Lr) beyond 30 years operation vs. AISI304 properties reduction [31] .....	42

## List of Abbreviations

AISI	American Iron and Steel Institute
ASME	American Society of Mechanical Engineers
ASTM	American Society for Testing and Materials
AT	Accelerated Thinning
ATH	Accelerations Time History
BRGM	Bureau de Recherches Géologiques et Minières
CMS	Conditional Mean Spectrum
CPU	Central Processing Unit
CVM	Control Volume Method
EPRI	Electric Power Research Institute
FE	Finite Element
IAEA	International Atomic Energy Agency
LTO	Long-Term Operation
LWR	Light Water Reactor
Lr	Residual Life
LWR	Light Water Reactor
NARSIS	New Approach to Reactor Safety Improvements
NPP	Nuclear Power Plant
PGA	Peak Ground Acceleration
PWR	Pressurized Water Reactor
RG	Regulatory Guide
RPV	Reactor Pressure Vessel
SG	Steam Generator
SOL	Service of Life
SSCs	Structures, Systems and Components
SSG	Specific Safety Guide
Tr	Residual thickness
Tm	Melting Temperature
Vs	Shear-Wave Velocity
WP	Working Package
Wr	Wearing rate

## 1 Executive Summary

A preliminary evaluation of the reliability of Gen III NPP components relevant for safety subjected to earthquake events and ageing was performed.

To account for the impact of cumulative effects by succession of events and ageing mechanisms in seismic fragility assessment of Structure, System and Component (SSC), a deterministic approach was adopted and several numerical simulations were performed by means of the finite element (FE) codes.

A 4500 MWth NPP, used as reference for this assessment, was being studied in the framework of the NARSIS (New Approach to Reactor Safety Improvements) H2020 project.

Section 4 and 5 present and describe the models, methodology and boundary conditions for properly accounting the cumulative effects caused by external events and ageing mechanisms. Regarding these latter, structural degradations due to plants' ageing, e.g. accelerated flow corrosion, creep and time and/or temperature material properties degradation, are among the key factors assessed to obtain a realistic evaluation of the class-1 safety structure (specifically reactor buildings and primary pipe), especially when extreme environmental demands, such as large earthquakes are considered.

Results from the several different analyses confirmed that ageing of structural elements is likely to degrade the mechanical performance and impair the structural capacity and reduce the residual safety margin. It emerged that ageing induces a reduction of the plant structural capacity by about 20%.

As for the primary pipe sub-structure, the thermo-mechanical loads resulted responsible for pipe deformation, which develops and increases as the transient progresses. Further, an excessive (general or local) wall thinning seemed to determine a dimensional change of the pipe, even causing bending or buckling.

Results allow to perform fragility analyses on the main critical elements of Nuclear Power Plants (NPP) as identified in task 2.3.

## 2 Introduction

In recent decades, the investigation of the way for continuing the operation of nuclear power plants beyond the time frame originally anticipated for their operation (typically 30–40 years) has steadily increased.

The long-term operation (LTO, see Figure 1) of NPPs, which may be defined as operation beyond an established time frame set forth by, for example, licence term, design, standards, licence and/or regulations, became a topic of growing interest as many countries using nuclear energy are committing also to ambitious decarbonisation targets (*Countries currently operating nuclear reactors will find in LTO of their plants a safe, ready-to-deliver and competitive option to support decarbonisation pathways, while reconciling the affordability and security dimensions associated with electricity provision [2]*).

Decisions regarding extending the operating licences for NPPs are complex and require the simultaneous evaluation of multiple factors among which the ageing phenomena and the possible effects and consequences they can cause on a NPP performance. The (re) evaluation of residual structural margin of this latter is mandatory of course.

A number of effects (e.g., components interconnections, components ageing, etc.) relevant to the safety analysis are generally not accounted for in the current methodologies for physical and functional fragility assessment. These effects may alter the general response of a NPP, due to a capacity reduction of the affected elements. For this reason, we propose to integrate some of these effects in the current methodologies used for seismic fragility assessment.

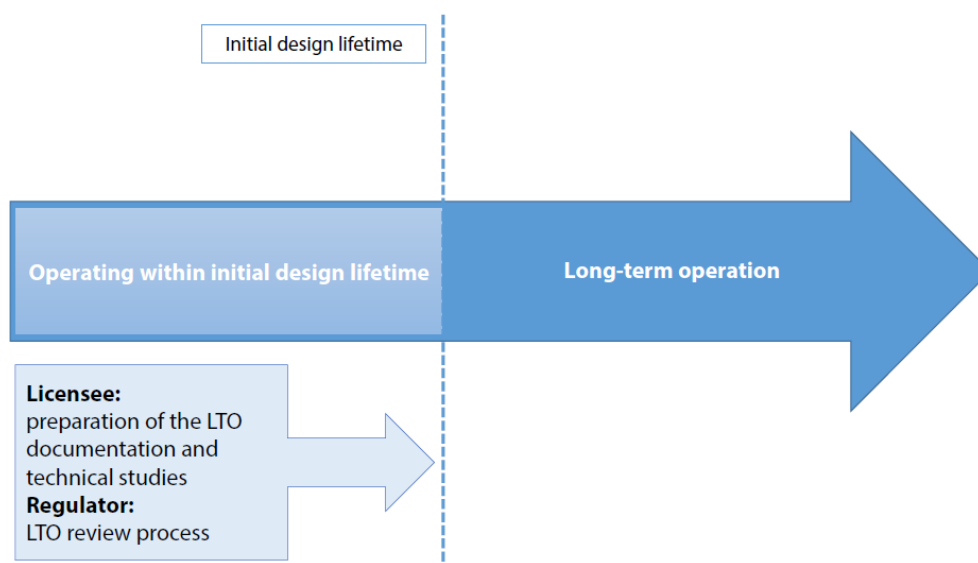


Figure 1: Generic definition of the time frame known as LTO period

As to the ageing, it requires not only addressing both the effects of physical ageing of SSCs, resulting in degradation of their performance characteristics, and the non-physical ageing (obsolescence) of SSC (i.e., they become out of date in comparison with current knowledge, standards and regulations, and technology), but also a comprehensive evaluation of the current conditions of the plant in order to identify issues that could arise during the foreseen LTO period.

While the main ageing mechanisms are generally common across all nuclear power plants, there can be specific concerns depending on the type of design, and the operational experience of the plant (Figure 2).

Having a clear and extensive understanding of the main ageing phenomena (see distinction provided below) related to life-limiting components in different conditions and nuclear systems

is hence key to support safe nuclear operations beyond the initial licencing period (enabling LTO). These phenomena may be grouped in:

1. **Physical ageing** is a general process in which the physical characteristics of SSC gradually deteriorate with time or use owing to physical degradation or chemical or biological processes (i.e. degradation mechanisms).
2. **Non-physical ageing** of SSC is the process of their becoming out of date (i.e. obsolete) owing to the availability and evolution of knowledge and technology, and the associated changes in requirements, codes and standards.

The evaluation of the cumulative effects of both ageing and obsolescence on the safety of a nuclear power plant is a continuous process and is required to be assessed performing a suitable equivalent safety assessment as ageing especially for plants with an average age of more than 30 years 7, may be responsible of a further reduction of the plant structural capacity.

During lifetimes, most of the plant SSC are replaced generally as part of normal maintenance procedures. There are, however, some of them, such as the RPV and concrete containment structures, for which the replacement may be unfeasible for technical and/or economic reasons. Consequently, an evaluation of critical life-limiting components is felt necessary to have a clear understanding of the main effects of the operational loads conditions on the components that shall guarantee the safe nuclear operations. And this becomes much more important when the occurrence of external events, such as the earthquake, is taken into account.

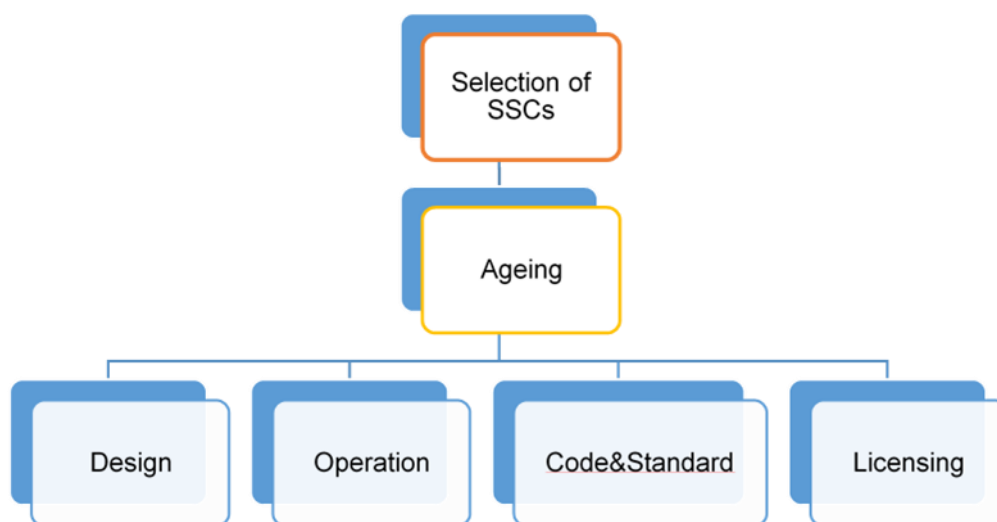


Figure 2: Integration of component-specific ageing with plant or system level analysis

In this study the effects of ageing on the seismic analysis of a Gen III NPP, that is required as one of the conditions for the design and construction approval, and on the performance of primary piping, are presented.

In the following, the methodological approach used to determine stressors will be described as well as the numerical simulations carried out. As for the piping performance concerned, several thinning type and rate have been considered, while as for the seismic analysis multistore approach has been applied.

### 3 Ageing

The IAEA NP-T-3.24 [5] also refers to the term ‘ageing’ to describe “the continuous time dependent degradation of SSC materials...” during normal service and transient conditions. As the components age, the plant original design ages too; this means that cumulative effects of ageing and obsolescence on the safety of nuclear power plants must be re-evaluated periodically to verify components (single component at small or whole plant at large [6]) performances are within acceptable limits. To that purpose accurate evaluation of the aging effects on through state-of-the-art models and application of the aging-management software is needed. In doing that, descriptive, operating and functional information and data and stressors have to be defined/determined.

Figure 3 shows the decrease of the safety margin as a function of the time: its analysis shows how important is to guarantee a minimum safety level, whatever the events that could occur. The existence of such level assures the safety margin at all times.

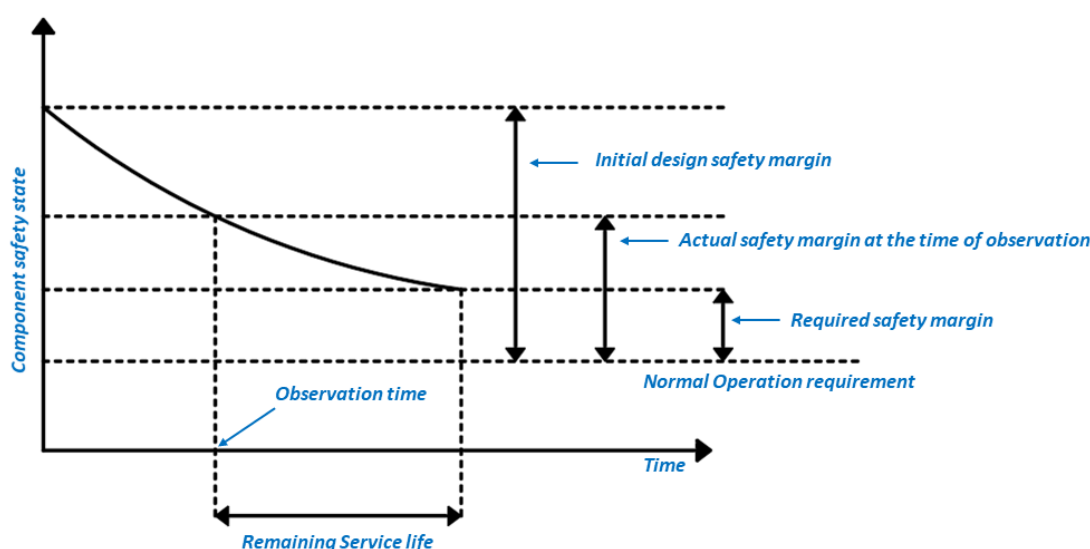


Figure 3: Conceptual component safety state

Understanding the SSC ageing, as shown in Figure 4, derives mainly from the knowledge of:

- The current licensing basis and anticipated updates to the licensing basis, where relevant (including regulatory requirements, codes and standards);
- The safety functions and other intended functions of the SSC;
- The design and fabrication processes used (including material properties, fabrication residual effects/defects, specific service conditions, results from maintenance, etc.);
- Any plant environmental conditions including neutron or gamma radiation fields;

To account for the “synergic effect” of the previous points, from (a) to (d), a procedure based on the IAEA systematic approach, which is provided in the below Figure 4, needs to be developed.

Owing to the complexity of ageing phenomena, a systematic and proactive approach should be adopted.

Ageing is a general deterioration process in which the characteristics of SSC gradually change with time and use. The service conditions, which contribute to ageing act mainly in two different ways: 1) through chemical and physical processes that affect material properties, and 2) through factors that can lead to the degradation of functional capability.

Exactly we may have [5] a degradation mechanism that:

- 1) affects the material internal microstructure or its chemical composition and thereby its ageing regression (e.g., thermal creep, radiation creep, irradiation damage, such as embrittlement, etc.);
- 2) imposes macro-geometrical damage to the component either through metal loss (e.g., corrosion or wear) or through cracking or distortion (e.g. stress corrosion, deformation or cracking).

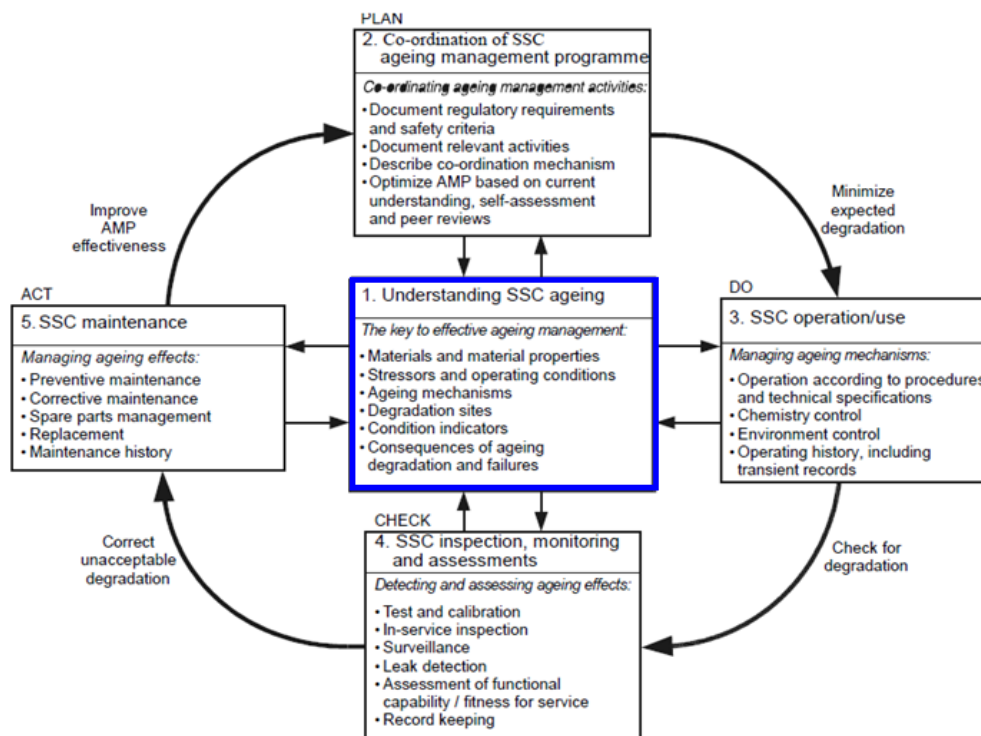


Figure 4: Systematic approach for ageing [4]

Aged SSC may thus undergo several changes in e.g., geometry, ductility, mechanical strength (Table 1).

Table 1: Main ageing mechanisms

Consequence	Degradation	Deformation	Embrittlement & Cracking	Material Loss
Degradation Mechanisms	Creep	Creep	Creep	
		Fatigue	Fatigue	
	Thermal Ageing		Thermal Ageing	
	Irradiation	Irradiation	Irradiation	
			Corrosion	Corrosion

It is worthy to remark that ageing is a problem not only for active components, whose likelihood of failure increases with time, but also for passive components, such as e.g., the containment building, whose protection margin is reduced to the lowest allowable level if not maintained. Figure 5 shows how the stressors, due to the several loading conditions, lead to a specific ageing mechanism and damage effects into the SSC materials.

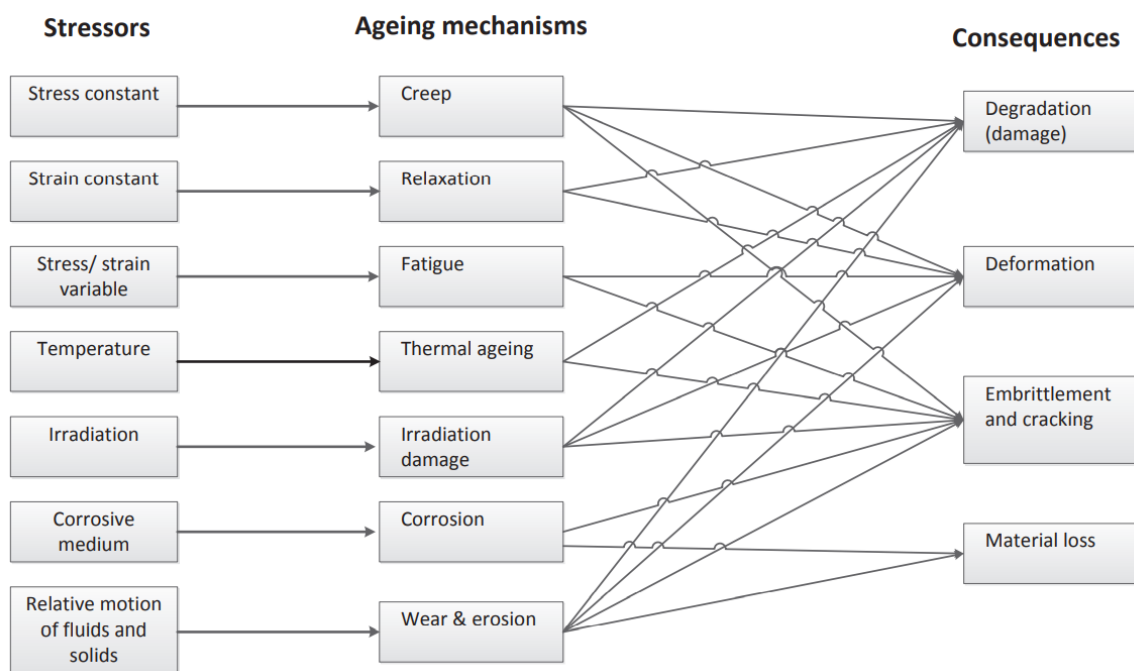


Figure 5: The most important ageing mechanisms and consequences for a NPP item (from [5])

The safety of NPPs could be affected by the age related degradation of key components or structures if it is not detected prior to loss of functional capability and if timely corrective action is not taken. The loss or even a reduction of functional capability of the key plant components could cause the impairment of one or more of the multiple levels of protection afforded by defence in depth, and in this way reduce the plant safety.

### 3.1 Effects of ageing on the integrity of plant

The reliability of the NPP physical barriers should be evaluated conservatively to ensure that the margins against failure of the plant safety component are retained. In fact, the ageing degradation of NPP components may lead to a higher probability of common cause failures due to the adverse impact on the effectiveness of the defence in depth, i.e., performance of the physical and engineering barriers: as an example, aged safety systems could fail simultaneously when subjected to abnormal conditions associated with a transient (e.g., high pressure, vibration, etc) associated with an operational upset or an accident.

Various ageing processes, even not detected and /or revealed during normal operation and/or maintenance, may gradually degrade the components, reduce design safety margins and cause failures of the safety SSC.

An example of a component whose ageing degradation could cause an increase in the probability of transients or accidents is a steam generator tube. The rupture could be caused by a large pressure transient in the primary system or by a severe earthquake.

### 3.2 Methodological approach for ageing

Since the performance of all plant components may be affected by ageing, there is a need to evaluate the effect that aged components have on system performance and plant safety.

Mathematical models of ageing processes and probabilistic safety assessment techniques can be used to determine how ageing affects SSC unavailability, identify plant components and systems that have a propensity to ageing and are risk significant, and to provide a quantitative assessment of the effects of ageing on plant safety.

Figure 6 shows the approach adopted for determining risk sensitivity to component ageing. It consists of three main phases: the first phase is aiming at determining the most critical component; the second phase is focused on the characterization of the ageing most degrading and deteriorating phenomenon; the third one is the performance assessment that is performed by adopting a deterministic approach and running numerical simulation (which are carried out by means of FE code).

Each phase is articulated in several sub-steps, among which:

1. Identify the critical SSC from the plant operation and safety point of view;
2. Identify the operational loadings, stressors, and ageing mechanisms with reference also to the type of material the component is made of;
3. Develop methodology for performance prediction;
4. Identify and implement points 1) and 2) in the deterministic FE codes;
5. FE assessment of the ageing effects and consequences for verifying the integrity of the structure or identifying the design improvement actions.

In particular, with reference to point 5) the root causes of the ageing deterioration, which can be environmental and/or operational dependent, have to be underlined. Either the former (material degradation over the time) or the latter (e.g., temperature and pressure gradient produced by transient conditions) need to be considered in the FE simulations.

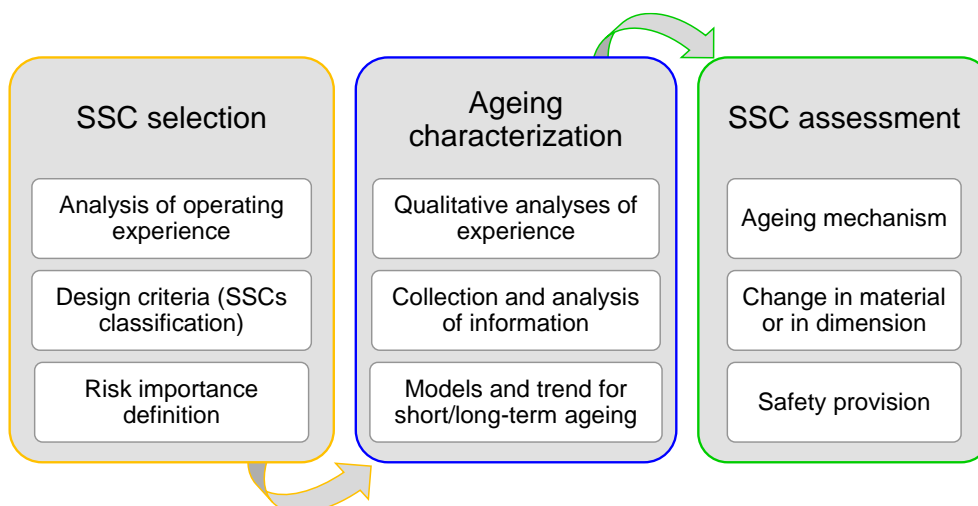


Figure 6: Approach for determining risk sensitivity to component ageing

The deterministic analysis should demonstrate that the plant safety requirements are met and that adequate margins (depending on the plant state) exist between the obtained values and the threshold values at which damage and failure start.

Conservatisms might be introduced in many ways, such as in acceptance criteria or through conservative assumptions in physical models or in initial and boundary conditions, which are defined based on the plant actual status.

Phase two of the above approach includes a sensitivity analysis that is performed with systematic variation of the key input variables to determine their influence on the results, and for demonstrating that realistically foreseeable changes in parameters do not lead to cliff edge effects. In addition, it includes validation aims at determining whether the mathematical models used in the FE code, through the equation of state, are an adequate representation of the real system being modelled. The deeper their knowledge, the more accurate the (numerical) evaluation. Moreover, by setting conservative bounds for initial and boundary conditions, it is so possible to minimize the parameter variability.

### 3.3 Referential NPP model

The 4500 MWth NPP, used as reference for this assessment, was being studied in the framework of the NARSIS (New Approach to Reactor Safety Improvements) H2020 project [7]. A generic (so-called “Gen”) III+ PWR equivalent to a 1300 MWe with large dry containment, proposed in NARSIS project (mainly WP2 to WP4), is considered for the development and verification of the proposed methodology and approaches.

The core is located inside the leak-tight RPV being a central part of the four cooling circuits (pressure boundary). The RPV is cylindrical, with a welded hemispherical bottom and a removable flanged hemispherical upper head with gasket. It is made of low-alloy steel (A304 austenitic steel is considered in this assessment). The complete internal surface of the RPV is covered by a stainless steel cladding for corrosion resistance. Its cylindrical shell consists of two sections, an upper and a lower part. The lower part is made of two cylindrical shells at the reactor core level, one transition ring, and one bottom head dome. The bottom head is a hemispherical shell connected to the RPV body through the transition: in the FE model continuity between the parts is assumed.

The internals located in the lower part of a RPV are: the core barrel, the lower core support structure, the neutron reflector, and the flow distribution device. These are vertically supported by a ledge machined into the flange of the RPV, the movement of which is constrained vertically to prevent them from lifting off the RPV ledge (see Figure 11).

Four pumps drive the flow, whereas the main heat sinks are four heat exchangers (SGs). The SGs are vertical shell, natural circulation, U-tube heat exchangers with integral moisture separating equipment. The tubes, made of Inconel 690, the perforated plates and the other internal components and the primary coolant, which are important for a correct definition of the thermo-structural-dynamic behaviour of the SG itself are represented through their stiffness and masses.

Figure 7 shows the main safety related systems and components of the containment building, extensive description of which is available in Del 4.1 of NARSIS.

Figure 7 (b) and Figure 8 show the vertical cross section of the containment system and RPV with overview of its main components, as lower core support plate, support system, barrel, etc., respectively. They report also the most important dimensions, based on which numerical models have been implemented.

The primary system is arranged symmetrically in the reactor building. Concrete walls are provided between the loops and between the hot and cold legs of each loop to provide protection against consequential failures. A water pool for storage of the upper core internals during refuelling is provided inside the containment for radiation protection.

The reactor building has a double concrete containment, consisting in an inner pre-stressed concrete containment with an integral steel liner and an outer reinforced concrete building. The reactor pit bottom connecting the RPV with the spreading area allows to collect and cool down the core debris.

Figure 9 shows instead the SG vertical cross section.

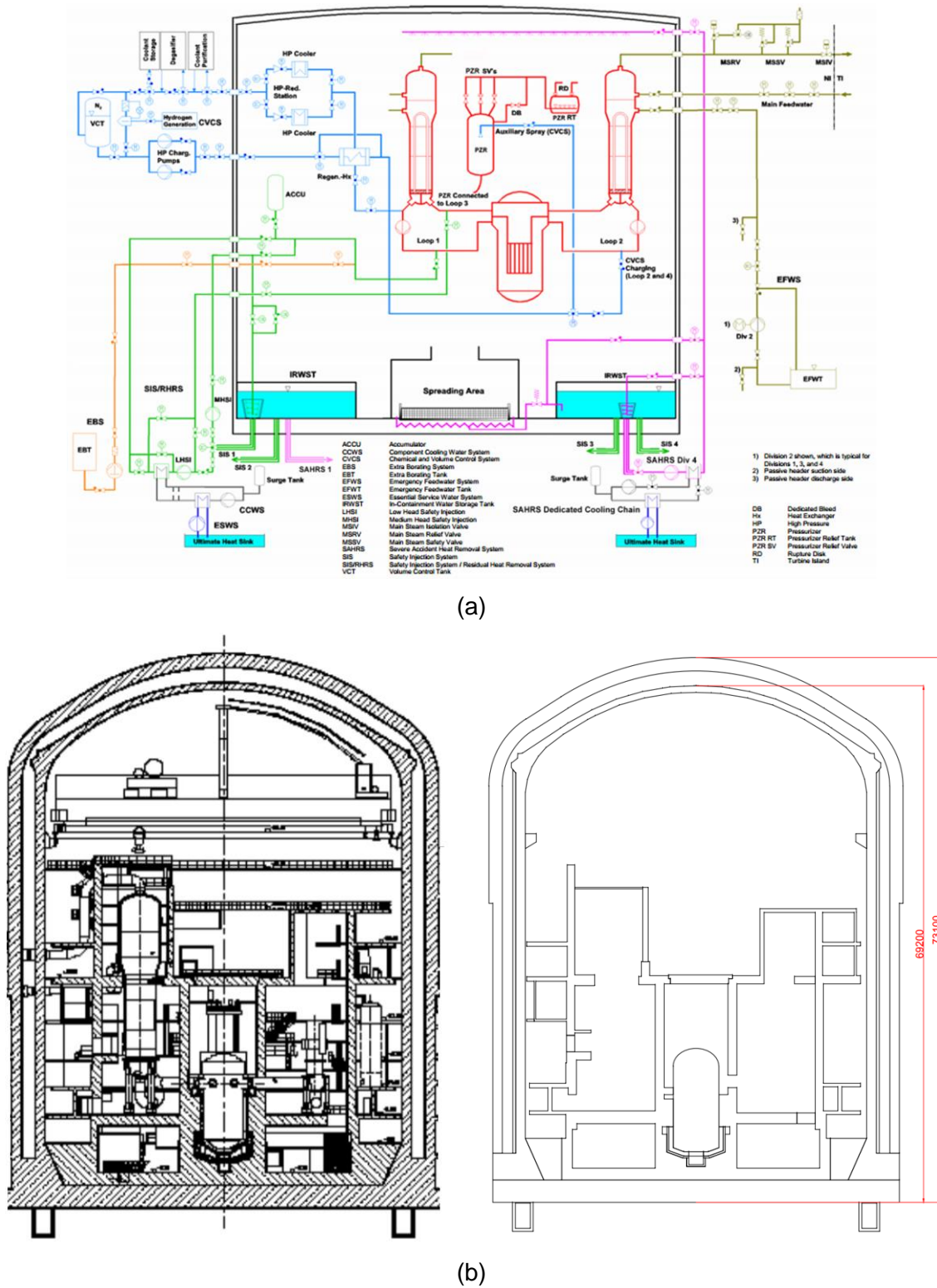
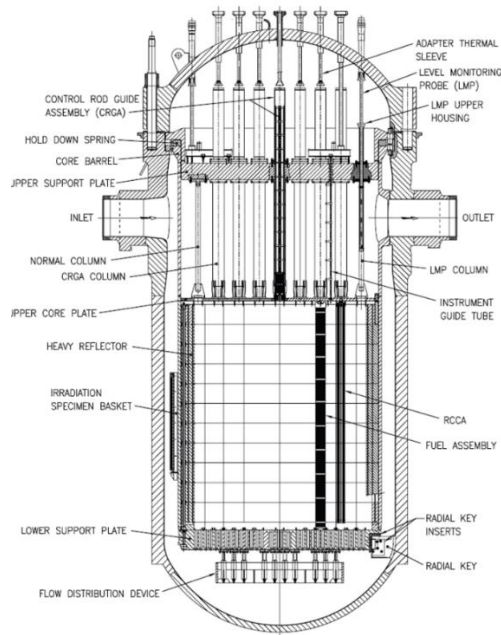
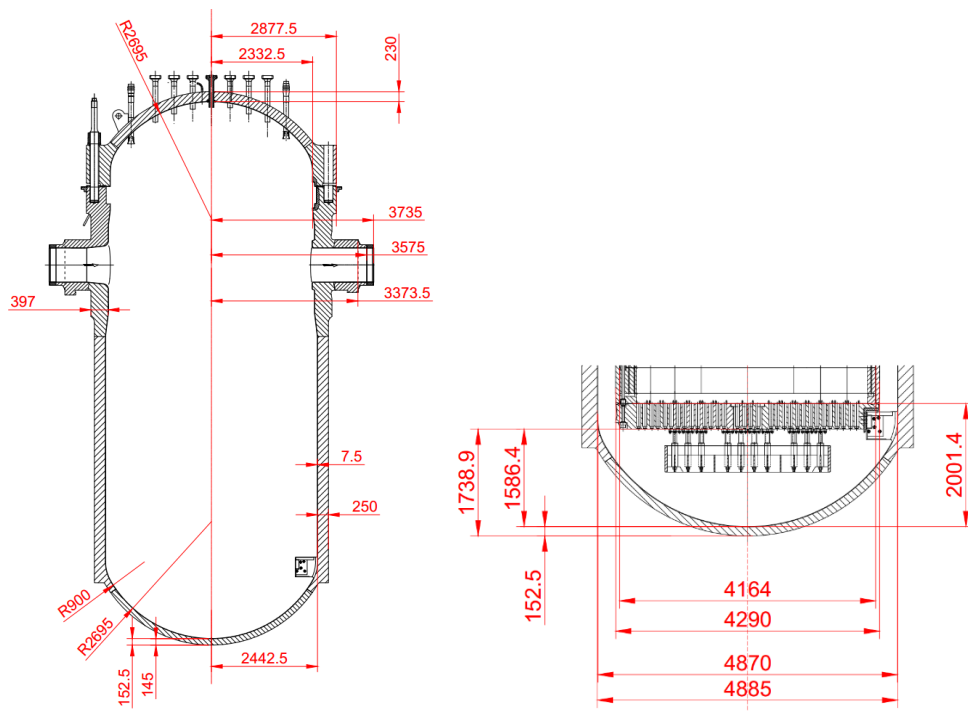


Figure 7: (a) Main SSCs of the generic PWR containment system and (b) vertical cross-sections of the double wall containment structure [mm]. The inner containment diameter is about 46 m



Vessel body weight	t	410
Vessel head weight	t	116
Weight of studs, bolts and washers	t	32
Total Mass of the RPV	t	526

(a)



(b)

Figure 8: (a) RPV vertical section with weight data [system unit: ton]; (b) RPV (left) and RPV lower head (right) with main dimensions [mm]

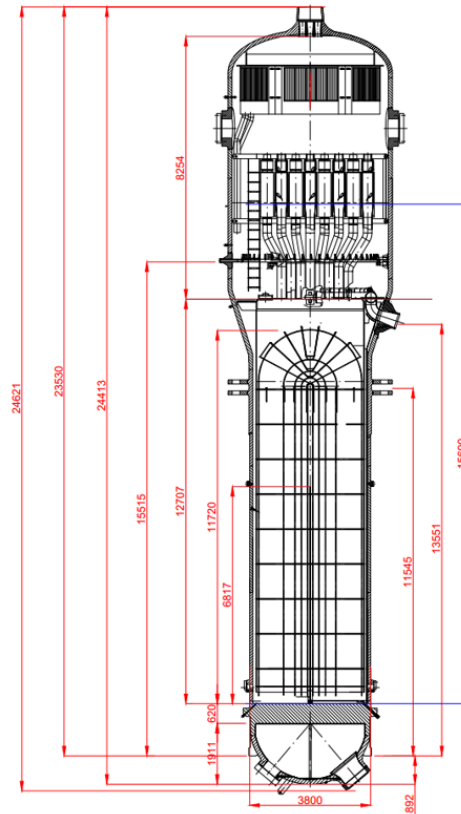


Figure 9: SG vertical section with main dimensions [mm]

Table 2 summarizes the main material properties used for the analysis of plant components behavior.

Table 2: Material properties of NPP components

NPP item	Young's Modulus [Pa]	Poisson's Ratio [-]	Yield Stress [Pa]	Density [kg/m <sup>3</sup> ]
RPV	2.1e+11	0.3	2.4e+08	7800
SGs	2.1e+11	0.3	2.75e+08	7850
Piping	2.1e+11	0.3	2.4e+08	7800
Containment	1.97e+10	0.25	5.6e+07	2000
Anchorage and supports	2.1e+11	0.3	2.4e+08	7800

In the next sections the investigations of an aged plant (30 years operation) facing operational and accident (seismic solicitation) conditions are presented and discussed.

## 4 Seismic investigation

Every year, 100,000 or more earthquakes that can be felt by people occur worldwide. These earthquakes range from very small to great and high magnitude (and catastrophic) earthquakes. The number of lives lost and the amount of economic losses that result from an earthquake depend on the size, depth and location of the earthquake, the intensity of the ground shaking and related effects on the building inventory, and the vulnerability of that building inventory to damage.

Today's design professionals know how to design and construct buildings and other structures that can resist even the most intense earthquake effects with little damage. However, designing structures in this manner can significantly increase their construction cost. Even in the areas of highest earthquake risk in the United States, severe earthquakes occur infrequently, often with 100 or more years between events capable of causing widespread damage. Given that many structures have, on average, useful lives of 50 years, constructing every structure so that it is invulnerable to earthquake damage would not be a wise use of society's resources.

Earthquake resistant design of structures requires realistic and accurate physical and theoretical models to describe the response of nuclear SSC that depend on both the ground motion characteristics and the dynamic properties of the structures themselves: to improve the plant design, and assess its vulnerability, the dynamic behaviour of structures subjected to critical seismic excitations that may occur during their expected/beyond service life must be evaluated.

This evaluation is complex and requires the knowledge and understanding of several factors, such as type and magnitude of the site-dependent earthquake event, NPP material behaviour, plant geometry, restraints fastening and/or anchorage system, ageing, etc.

### 4.1 FE model description

The standard design of a LWR refers to an envelopment of site conditions such that the NPP would be suitable for construction on any given site without necessity of site specific analysis and design. As indicated in Sect. 3.3, a generic III+ PWR equivalent to a 1300 MWe with large dry containment is considered. (vertical section of the considered PWR plant is shown in Figure 7 b, characteristics and technical details of which are described in Del. 4.1 of [7]).

The plant was assumed as founded on rigid foundation at the base, which joints the inner structures to the top soil deposit [8][9]. The containment of this reactor system consists of an outer containment and an inner containment. The outer containment shell is a reinforced concrete structure with large wall thickness and protects the inner containment from direct effects of external hazards.

The leak-tightness function is ensured by a steel liner on the inner surface of the containment that is anchored in the inner containment wall by L-profiles (so-called "continuous anchors") and by headed studs. The inner containment structure consists of the base slab, the cylindrical part and the dome part. The base slab is connected to the cylindrical part by the gusset area in which the wall thickness increases considerably.

Cylindrical and dome part are joined by a ring beam, the function of which is to withstand the bracing forces caused by the dome and to enable the tendons anchoring.

The cylindrical part has an inner diameter of about 46 m. The wall thickness of the dome part is about 1.0 m. The total height from the basement to the dome centre of the external containment is about 73 m.

High strength class for both concrete and steel reinforcement is considered [10][11]: the tensile stress value is about one-tenth to one-fifth the compressive strength ( $5.6e+07$  Pa) for concrete.

Steel reinforcement consists of plain carbon steel bar that typically conforms to ASTM A615 or A706 specifications. The minimum yield value of A615 ranges from 280 MPa (Grade 40) to 520 MPa (Grade 75), while 420 MPa (Grade 60) is the most common value considered for steel bars.

Steel reinforcement is also used in compression members to safeguard against the effects of unanticipated bending moments that could crack or even fail the member. Therefore the effectiveness of reinforced concrete as a structural material depends mainly on the interfacial bonding between the steel and concrete and on their thermal expansion.

The containment openings, such as the equipment hatch, the fuel transfer tube, pipe, and cable penetrations, etc. were considered through a reduced equivalent area of the cross section.

In the set-up model all the RPV and the SG internals, as well as the water inventory, were considered as a set distributed masses linked respectively to their reference location within the containment system.

Lumped masses were also introduced in the model to represent some component; to reduce CPU calculation time and mainly for providing accurate representation of the dynamically significant modes of vibration these components.

All the main primary coolant system components (core reflector/shield, pressurizer, reactor coolant pumps, steam generators, and control rod drive mechanisms, etc.) are located inside the RPV and represented through their weight.

The previous Table 2 summarises the main mechanical material properties of the SSC implemented in the NPP model, while Table 3 those for rebars (A 615 grade 60).

Table 3: Steel rebars properties

Material property	Value
Density [kg/m <sup>3</sup> ]	7800
Young's Modulus [Pa]	2.1 E+11
Poisson ratio [-]	0.3
Yield Stress [Pa]	375-420 E+6
Elongation to Fracture [%]	> 14

All the material properties were assumed to be time independent. Moreover in the deterministic analyses performed, ageing was considered by assuming a constant reduction of material properties (e.g., strength,  $\sigma$ , or Young' modulus, E, etc.) representative of 30 years' operating life of plant.

According to the IAEA SSG-2 (Rev. 1) [12], conservative assumptions were made in the analysis concerning the availability of plant systems included:

- (a) Normal operation systems that are in operation at the beginning of the postulated initiating earthquake event
- (b) No safety or mitigating system operation.
- (c) Safety features specifically designed for design extension conditions should not be credited in the analysis.

## 4.2 Seismic analysis

To proceed with the verification of earthquake resistant structures, a deterministic approach is adopted, in the first step [13]. A goal was to develop a representative model of the reference NPP structures, in order to closely simulate their dynamic behaviours as accurately (and completely) as possible.

Figure 10 shows the whole 3D model implemented in the item's element (FE) code MSC.MARC [ref], which is a powerful tool for nonlinear analysis of item behaviour under dynamic and multi-physics loading scenarios.

Figure 11 shows the sub-model of the four SGs with joint piping. The figure shows the four support legs or columns hinged to ball-jointed brackets (to allow the SG to move freely and accommodate the primary loop temperature variation), and the lateral supports guide that restrain the SG movements during accident events. Moreover, the SG is assumed to be restrained rigidly on the inner reactor containment internal basement floor.

The whole model consists of more than 130,000 solid elements. Elements' types are thick shell, solid brick, and solid section beam with global displacements and rotations as degrees of freedom. For these elements, stiffness is calculated at their own Gaussian integration points. These models will form the basis for all subsequent dynamic transient analyses.

Indeed the adopted mathematical model and the degree of FE models' discretization were chosen such that the natural behaviour of the structure in the relevant frequency range could be computed with good reliability.

The behaviour of concrete was assumed to be linear elastic up to the point of failure. During a seismic event, the structural components may be subjected to repeated cyclic load reversals and combined axial, flexure, and shear effects. Therefore, they may undergo inelastic deformations during the severe ground shaking caused by major earthquakes. As a result of accumulated damage during inelastic excursions, the seismic response of reinforced concrete structures may exhibit stiffness degradation and strength deterioration. Consequently, to simulate properly their behaviour, a material degradation method was taken into account in compression and in tension.

The model damage is a continuum, plasticity-based, model for concrete is associated with main two failure mechanisms that are the tensile cracking and compressive crushing. The concrete damaged plasticity model provides a general capability for modelling concrete in all types of structures (beams, trusses, shells, and solids) and uses concepts of isotropic damaged elasticity in combination with isotropic tensile and compressive plasticity to represent the inelastic behaviour of concrete. Compressive stiffness is recovered upon crack closure as the load changes from tension to compression, but the tensile stiffness is not recovered when the load changes from compression to tension.

It should be noted that the recovery of stiffness affects bending dynamic behaviour of the damaged structure. The behaviour of the steel reinforcements, which were embedded into the concrete walls, was assumed to be elastic-perfectly plastic. The thickness of the steel bars has been determined by assuming that their cross-sectional area are uniformly spread along the respective pitch of the layers.

The equivalent Von Mises yield criterion and the piecewise linear method have been adopted to describe the plastic behaviour.

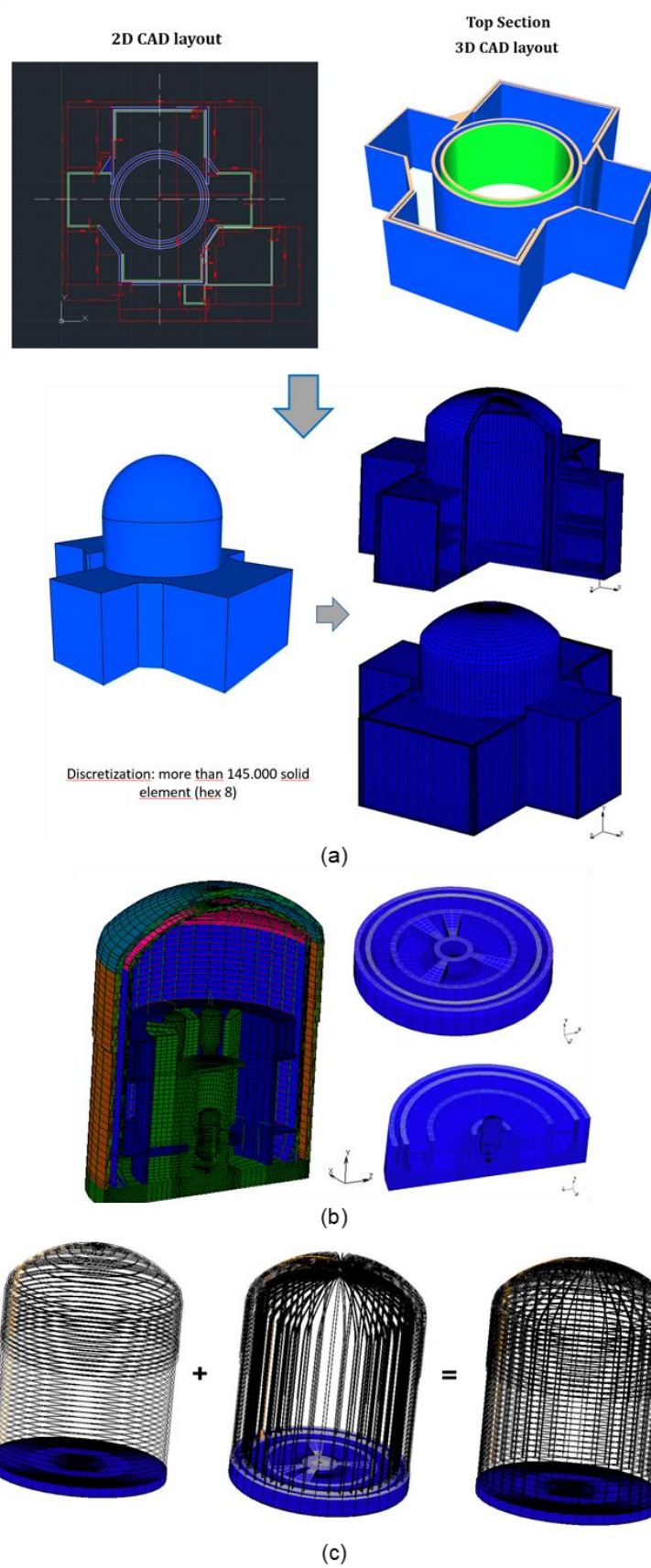


Figure 10 a, b, c: Overview of the geometrical model and FE model of Gen III NPP (a). In (b) the containment system, and in (c) the horizontal and vertical steel reinforcement arrangements are shown.

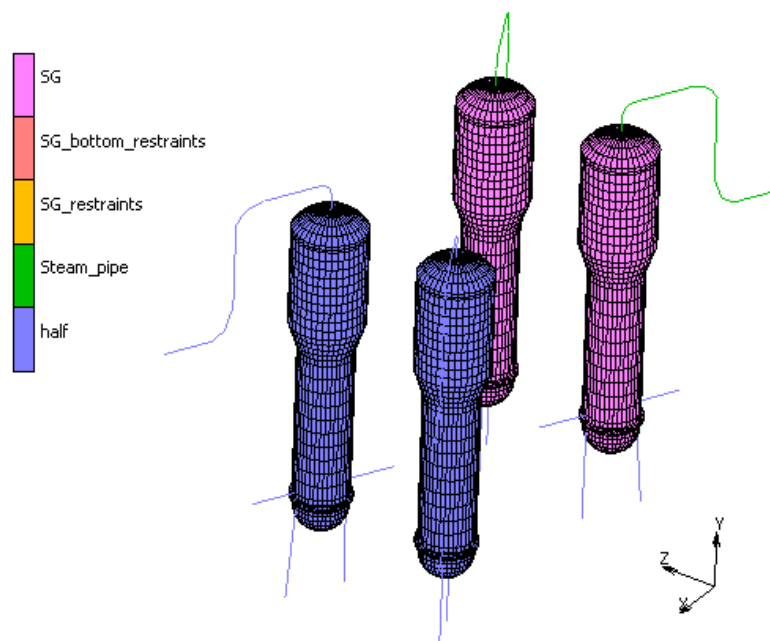


Figure 11: Detail of the NPP model: arrangement of 4 SGs, bottom and lateral lower supports included, and piping. The term half identifies the symmetric part of the systems

#### 4.2.1 Numerical simulations

After having adequately modelled the main structures in 3D FE models, the seismic analysis was carried out by adopting the time history approach [13].

The input acceleration data were provided in forms of time histories of accelerations (ATHs) calculated for an appropriate soil damping input ground motion provided at surface level. For the purpose of the seismic response analyses, we used 50 records calculated based on the conditional mean spectrum (CMS) [14].

Each input ATH (provided by BRGM) was obtained from the hazard-site seismic disaggregation analysis for a time-averaged shear-wave velocity to 30 m depth ( $V_{s30}$ ) of 800 m/s.

In doing that, site categorization has been considered as [15]:

- Type 1 sites:  $V_s > 1,100$  m/s;
- Type 2 sites:  $1100$  m/s  $> V_s > 300$  m/s;
- Type 3 sites:  $300$  m/s  $> V_s$ .

$V_s$  is the best estimate shear wave velocity of the foundation medium just below the foundation level of the structure in the natural condition, for very small strains.

Sets of mutually orthogonal and statistically independent artificial time history accelerations were used simultaneously as input for the dynamic transient analysis: two horizontal component and one vertical component, in agreement with the R.G. 1.92 rule [16].

The duration of each input ground motion and transient analysis performed is 20 s; the timestep of the transient analysis was 0.01 s.

Before the development of the dynamic transient analysis, modal analyses were carried out to evaluate the natural dynamic behaviour of structures by means of frequencies and modes of all the most relevant components of the considered system with a sufficient number of modes. The understanding of the dominant modes of the plant structures allowed to calculate Rayleigh damping coefficients implemented into the FE model to account for the structural damping.

All seismic transient analyses were performed assuming a proportional damping for each structure, in according with the equivalent Rayleigh damping [14].

The dissipation of energy of the vibrating structure is represented with decoupled equations that approximate the damping matrix by a linear combination of the mass and stiffness matrices. The damping matrix [C] resulted from a combination of the mass and stiffness matrices:

$$[C] = \alpha [M] + \beta [K]$$

Where:

[M] is the mass matrix of the structure;

[C] is the damping matrix of a physical system;

[K] is the stiffness matrix of the structure;

$\alpha$  and  $\beta$  are predefined constants.

If a natural frequency  $\omega_i$  and a modal damping ratio  $\xi_i$  are selected, the mass and stiffness matrix multipliers for damping,  $\alpha$  and  $\beta$ , should satisfy the following Rayleigh equation:

$$\xi_i = \frac{\alpha}{2\omega_i} + \frac{\beta\omega_i}{2}$$

For given damping ratios ( $\xi_1$  and  $\xi_2$ ) and frequency range ( $\omega_1$  and  $\omega_2$ ) the predefined constant values can be computed as:

$$\beta = \frac{2\xi_2\omega_2 - 2\xi_1\omega_1}{\omega_2^2 - \omega_1^2}$$

$$\alpha = 2\xi_2\omega_2 - \beta\omega_2^2$$

Mass and stiffness damping may be used to represent the energy loss due to impact and the rate of deformation forces. Damping ratios of materials for building of height >50 m are from [17].

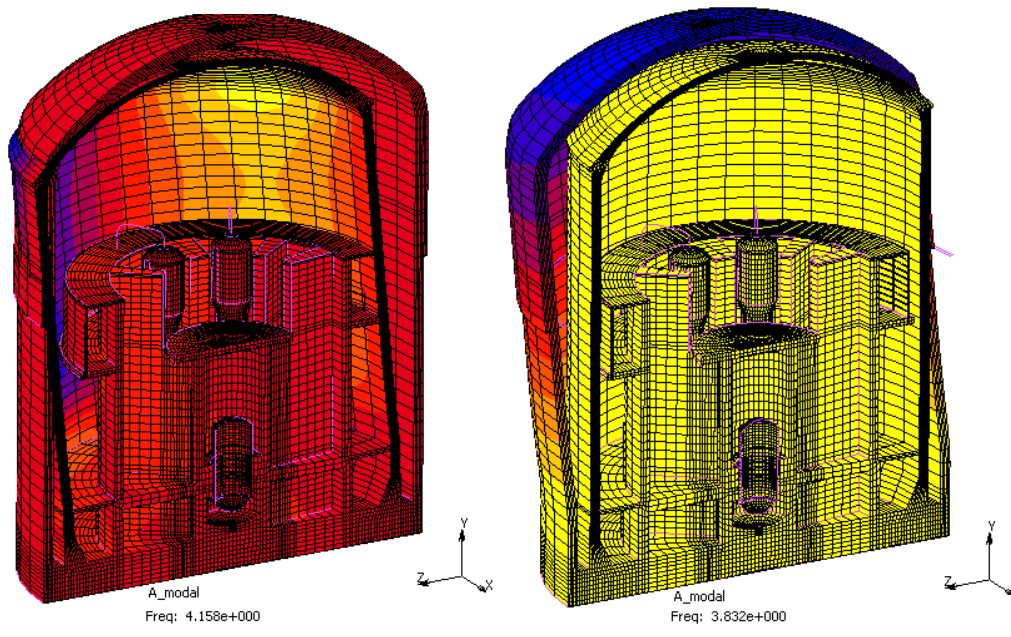
#### 4.2.2 Modal Analyses

Before performing transient analyses, modal analyses were carried out to evaluate the natural frequencies and modes of all the most relevant components in order to predict/describe the natural dynamic behaviour of reactor building structures. The natural frequency values and modal shapes provide information on the seismic response characteristics, such as amplification factor, which is strictly related to the energy dissipation or damping effects of each material, and expected displacements.

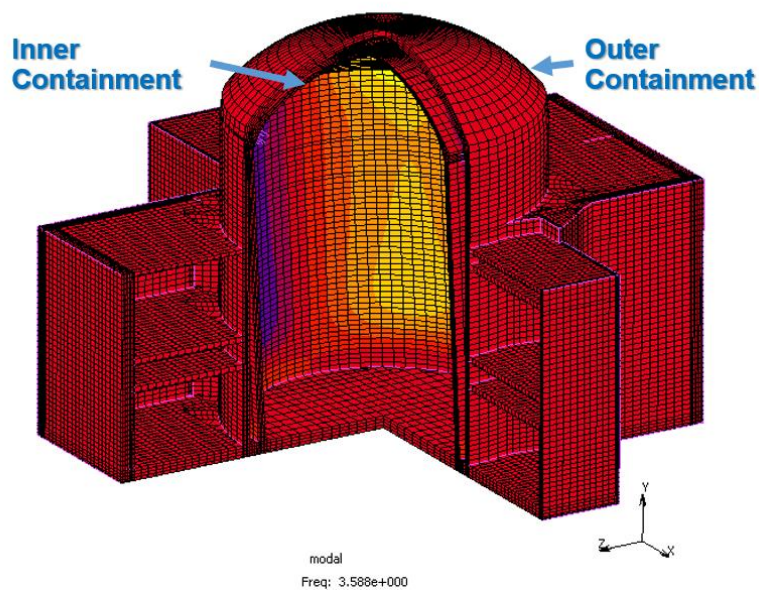
The modal shapes of the reactor buildings are shown in Figure 12, which corresponded respectively to the “beam mode” (translational/horizontal direction along z axis).

Figure 12 (b) shows the same frequency and eigenvector (or modal shape) of the outer reactor containment as obtained from the modal analysis carried out on the overall plant. Table 4 provides the dominant frequency of the important structures discretised in the set up and implemented within FE model.

It is worthy to note that the non-structural components, such as interior partitions or water inventory, etc. did not significantly influence the modal behaviour of the overall reactor building; they only contribute to the initial mass and global stiffness.



(a)



(b)

Figure 12: First modal shape of the outer and inner reactor containment, respectively. In (b) the results of the modal analysis carried out on the overall plant confirming that the 1<sup>st</sup> “cantilever” mode outer reactor containment is at about 3.6 Hz

Table 4: Modal analysis results

Mode #	Frequency [Hz]	Description
1	2.89	1 <sup>st</sup> “cantilever” mode of SG
2	3.84	1 <sup>st</sup> “cantilever” mode outer reactor containment
3	4.17	1 <sup>st</sup> “cantilever” mode inner reactor containment
4	25.02	1 <sup>st</sup> “cantilever” mode of RPV

### 4.2.3 Transient Analysis

To perform transient analyses a direct integration method employing a finite difference approximation was used. The unconditionally stable Newmark's implicit integration method was adopted for the solution of the dynamic equilibrium equations as well as the unconditionally stable average acceleration integration scheme with  $\gamma=0.5$  and  $\beta=0.25$ , where  $\gamma$  and  $\beta$  are the parameters used to control the accuracy and stability of the method of integration.

The Newton Raphson iteration scheme allowed to carry out iterative corrections to the displacement increment for solving the non-linear equations of equilibrium.

The results obtained from the simulations in form of accelerations along/inside the reactor building structure (specifically calculated at the monitoring points indicated in Table 5 show that acceleration amplifies along the containment height, as expected.

Table 5: Monitoring points location

Structure	Nodal point Id.	Global coordinate system [m]		
		x	y (vertical axis)	z
SG4	10023	-9.94	-7.77	13.69
Inner containment	36762	18.47	28.56	-9.41
	60348	13.58	28.07	18.69
Inner containment roof	89438	0	58.34	2.88
Pipe-SG connection	98307	-9.66	30.43	-49.22
	98415	-10.91	29.74	-3.21

The amplification was greater especially in correspondence of the dome cross-section, where, considering the model assumptions, it can be 3 to 4 times higher than the input ground motion ( $V_{s30}$  of 221 m/s), due to the overall containment building flexibility in the entire range of frequency of the earthquake.

Figure 13 shows the plots of the acceleration of the worst simulation case, which was characterised by this amplification.

The plots of the accelerations were obtained at several monitoring points in/along the internal containment cylindrical to identify the structural weak part of the unaged structure.

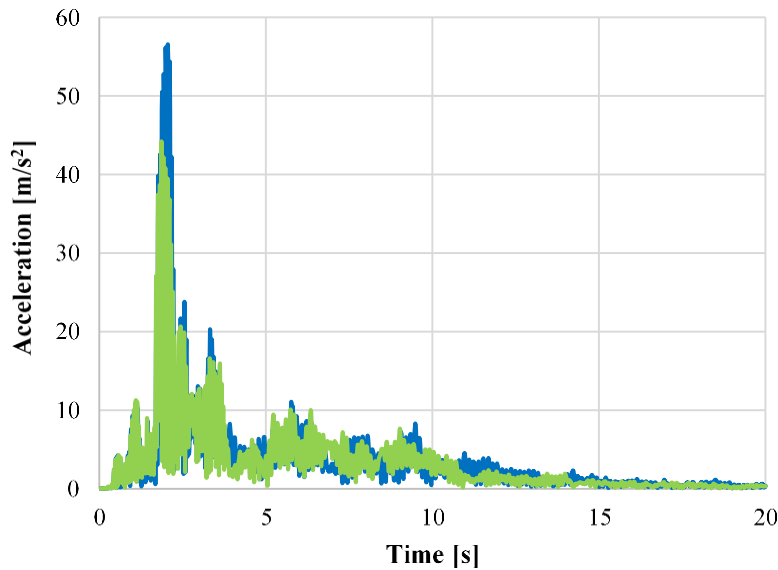
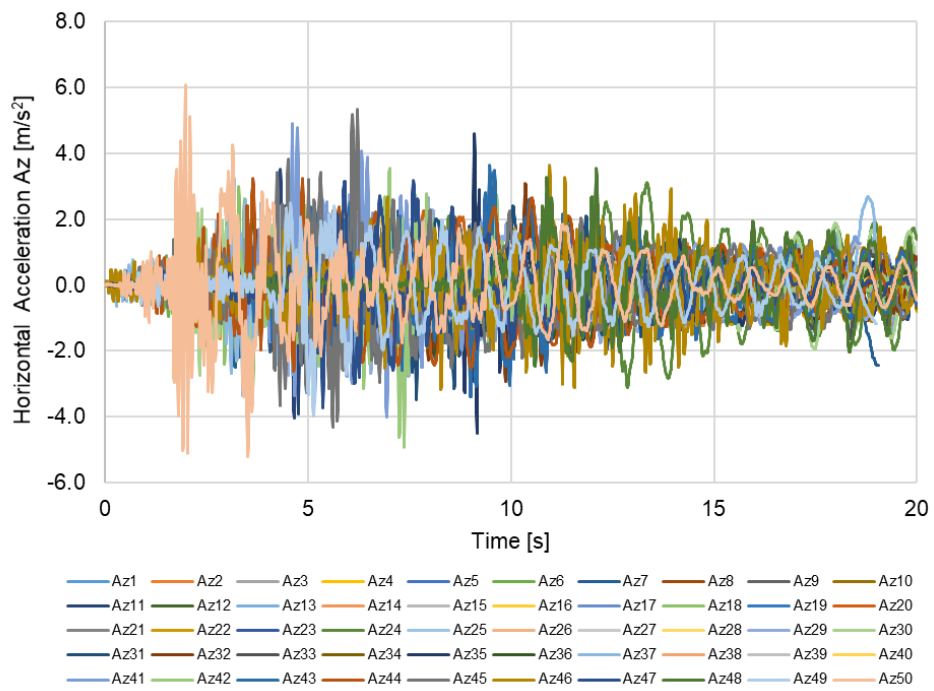
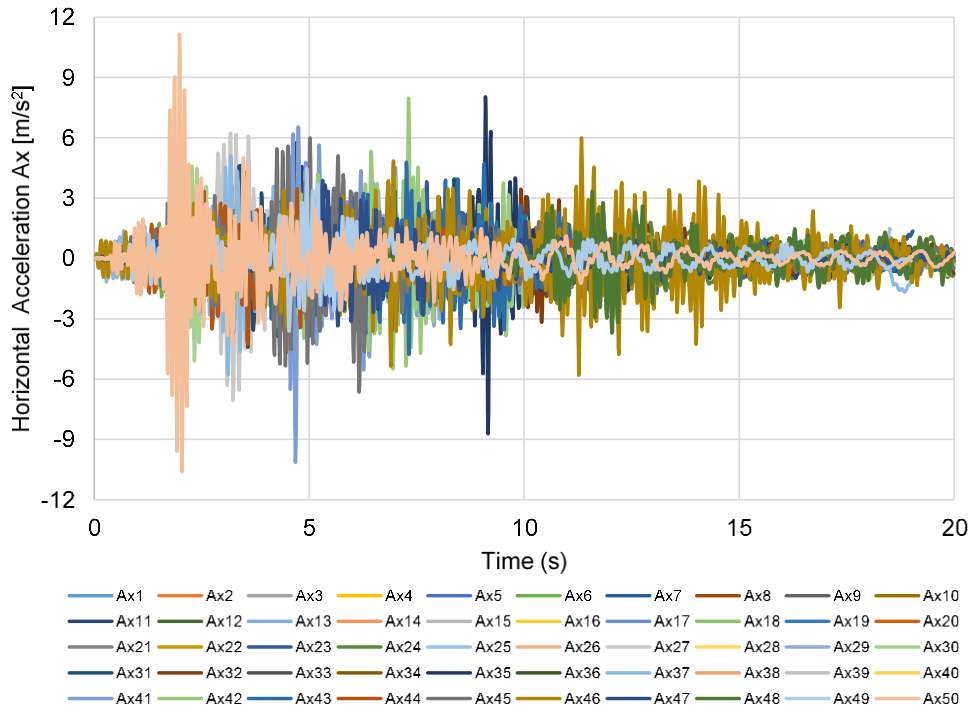
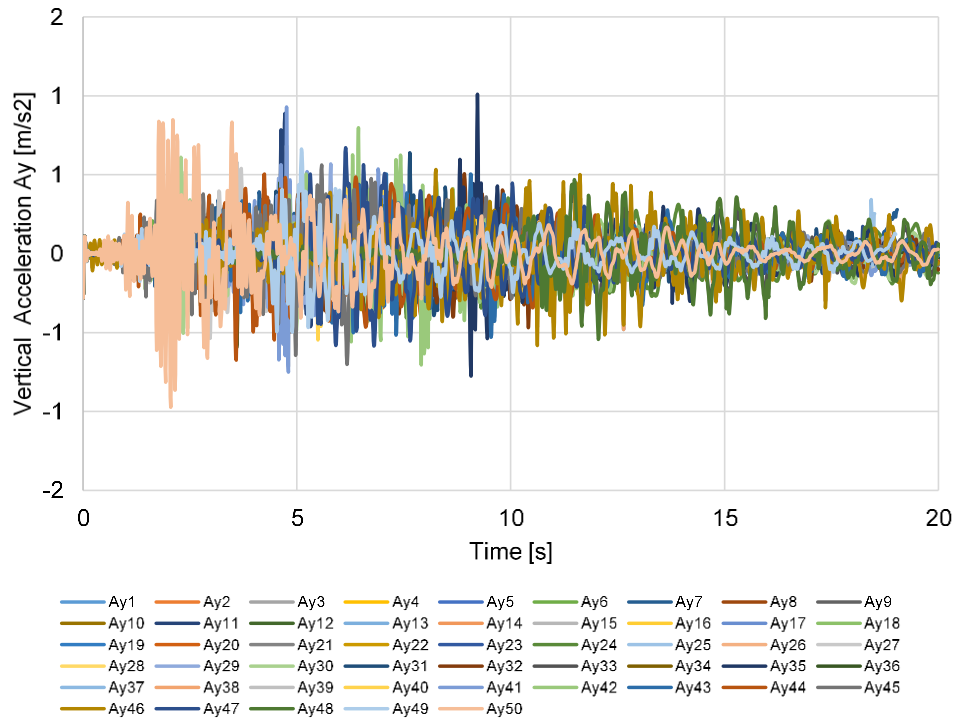


Figure 14 and Figure 15 show the comparison of acceleration and equivalent stress of Von Mises for both aged and unaged NPP, respectively, for the only monitoring point located at the roof of the internal containment. Example of the acceleration and stress counter plots are provided in Figure 16 and Figure 17, respectively.

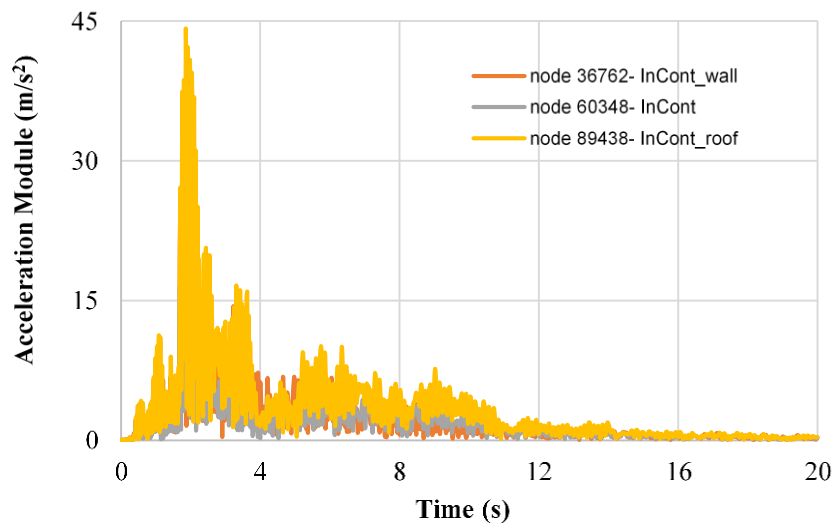
The degradation of the material, prolonged over the time, results in a detriment of structural capacity of the plant. This may suggest that local loss of stability could occur. The plots of the equivalent Von Mises stress (Figure 15) confirm that the greater the reduction of the material strength, the larger the damage suffered by the concrete. Although the local stress is close to the limit strength, the mean stress value was below the one that could determine the failure of the internal containment.

As for the relative horizontal displacement (Figure 17), it may reach a mean value of about 12 mm at e.g. SG elevation, suggesting that structural problems may arise for piping and penetrations.





(a)



(b)

Figure 13 a, b: (a) Horizontal and vertical ATHs calculated at the node 98415, representative of the connection between pipeline and SG4, as an example. (b) Module of the acceleration for ATH50

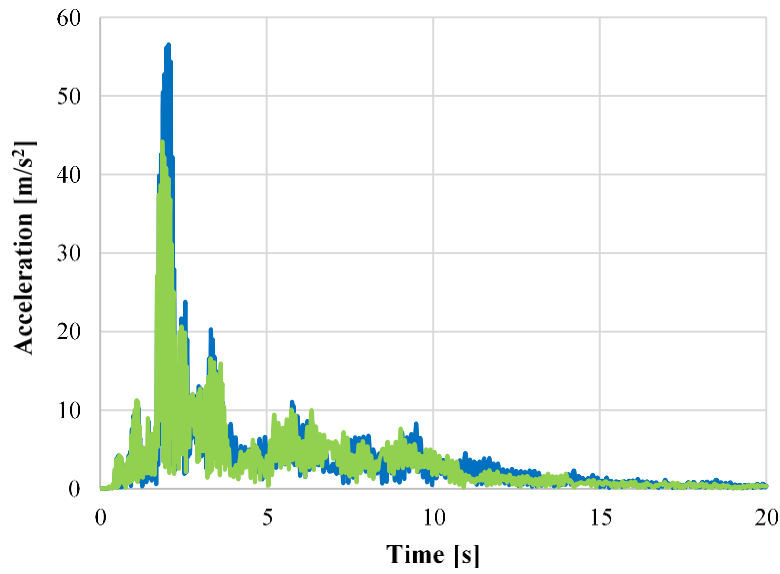


Figure 14: Acceleration comparison for ATH50 between aged (blue curve) and unaged (green curve) NPP at the internal containment hemispherical roof wall.

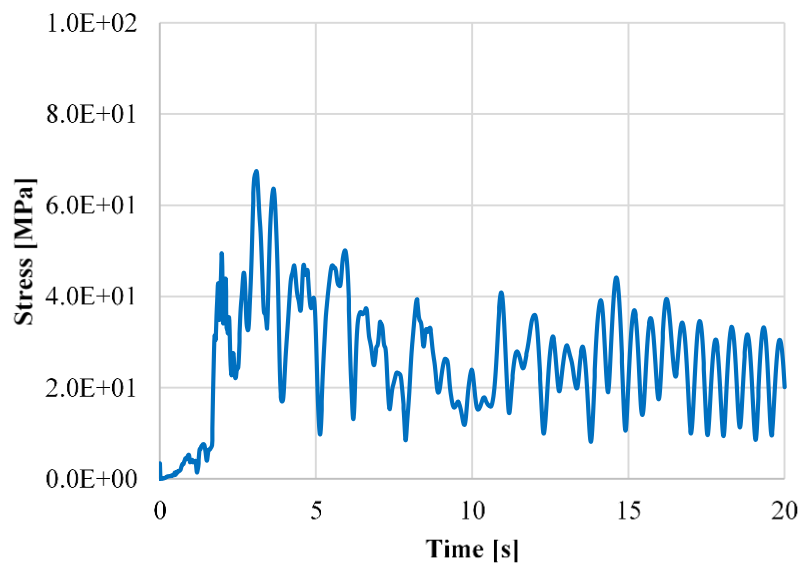


Figure 15: Example of Von Mises stress comparison for ATH50 between aged (blue curve) and unaged (green curve) NPP at the internal containment hemispherical roof wall. For ageing assessment temperature dependent material properties were taken into account.

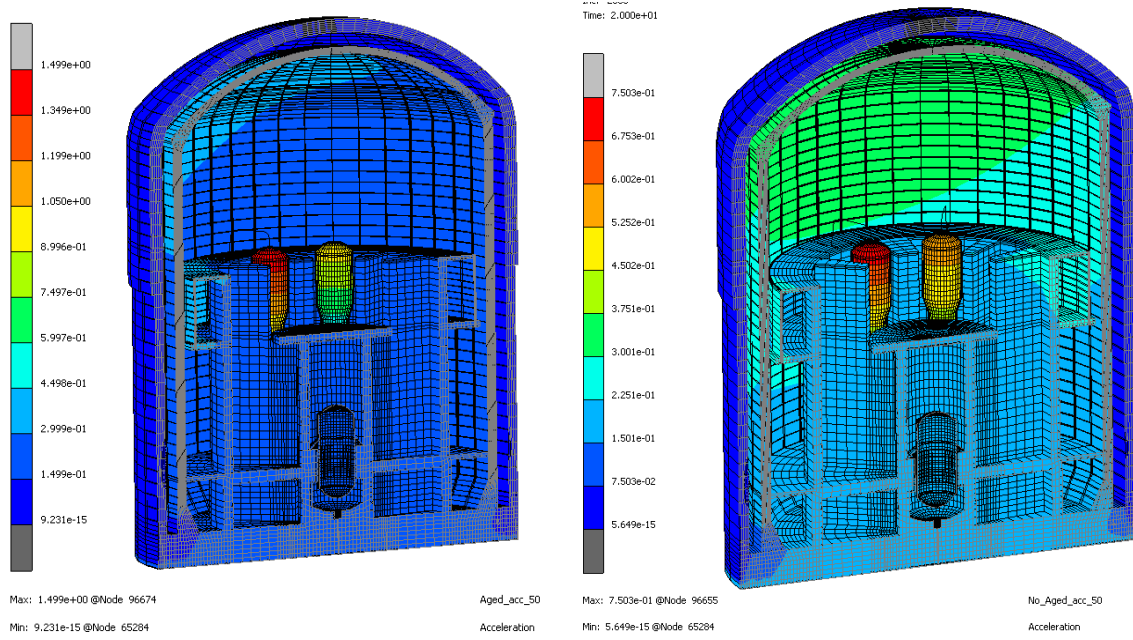


Figure 16: Example of acceleration counter plot for ATH50 input for aged (left) and unaged (right) at  $t=20s$

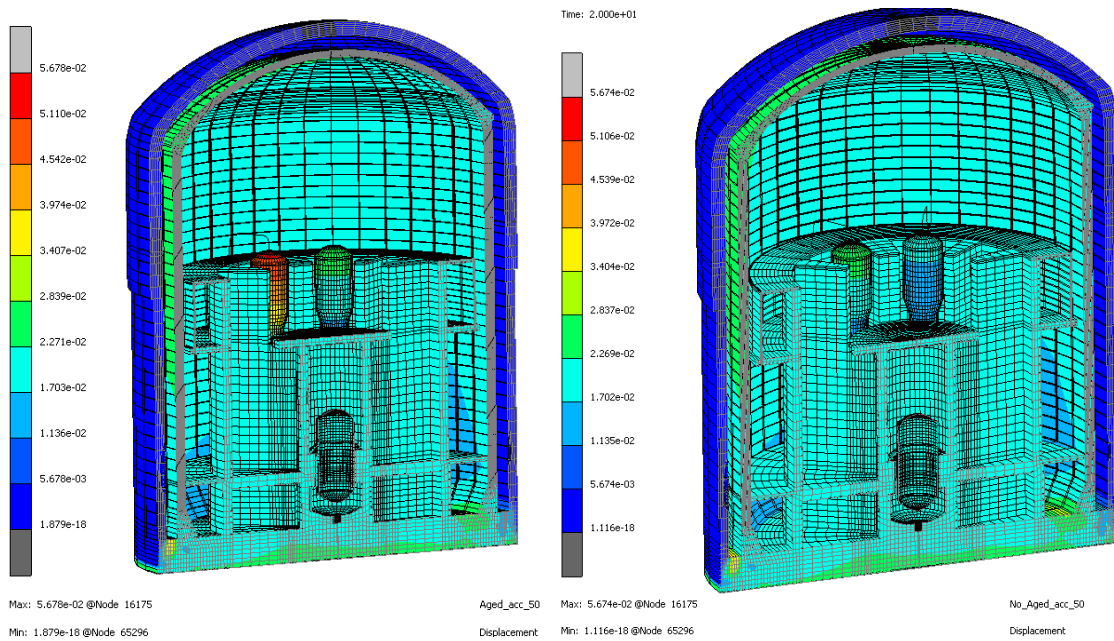


Figure 17: Example of displacement counter plot for ATH50 input for aged (left) and unaged (right) at  $t=20s$

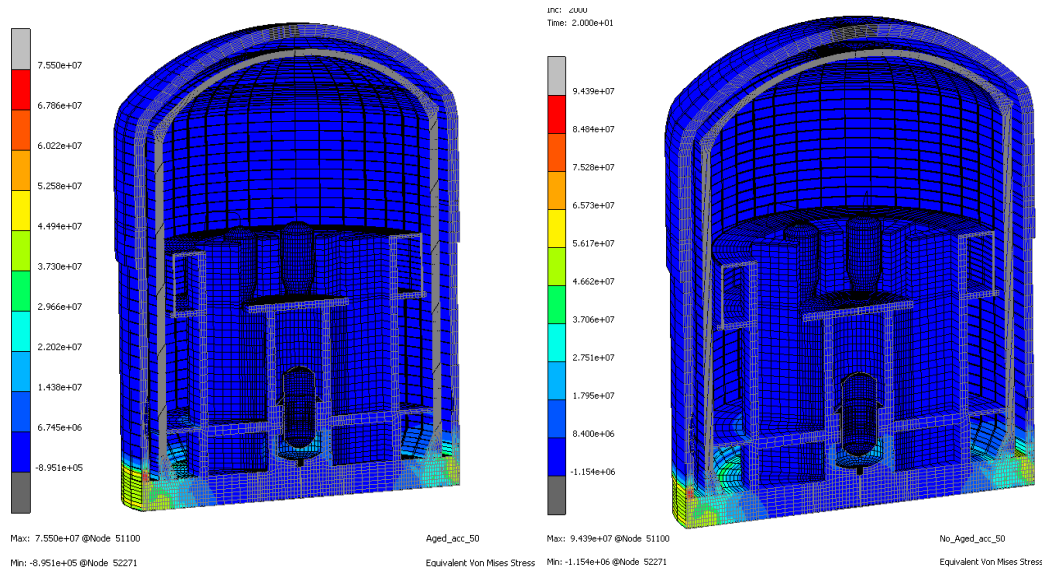


Figure 18: Example of equivalent stress counter plot for ATH50 input for aged (left) and unaged (right) at  $t=20s$

### 4.3 Main conclusions

A preliminary evaluation of the reliability of a generic Gen III NPP, for the configuration and assumptions made, subjected to earthquake events, having different PGA and acceleration vs. frequency content, was carried out taking also into account the influence of the ageing.

The seismic simulations were performed by adopting a deterministic approach and using a qualified FE code for this purpose.

Results show the following points:

- The greatest amplification of the seismic loadings occurred for an ATH input with  $V_{s30}$  of 221 m/s.
- The acceleration at the dome of the internal containment was 4 times higher than the input ground motion
- The equivalent Von Mises stress confirmed that the greater the reduction in material strength because of ageing, the greater the reduction in the structural capacity and the larger the damage suffered by the concrete.
- The mean value of relative horizontal displacement was about 12 mm at e.g. SG elevation, suggesting that structural problems may arise for piping and penetrations.

## 5 Aged primary piping analysis

Aging analyses is performed and presented in this section on the primary piping substructure in order to quantify the effect of the extended operation period on the structural integrity of Class I SSC. Specifically, a thermo-mechanical performance assessment is carried out considering thermal degradation phenomena and thinning [18][19][20].

Thinning (homogeneous or localized- heterogeneous), due to the operation of the nuclear plants, determines a progressive reduction (few tens of  $\mu\text{m}$  per year) of the thickness of the pipe (the developed and adopted approach is shown in Figure 19). If the thickness is reduced too much, the pipe may collapse under the internal pressure [21][22].

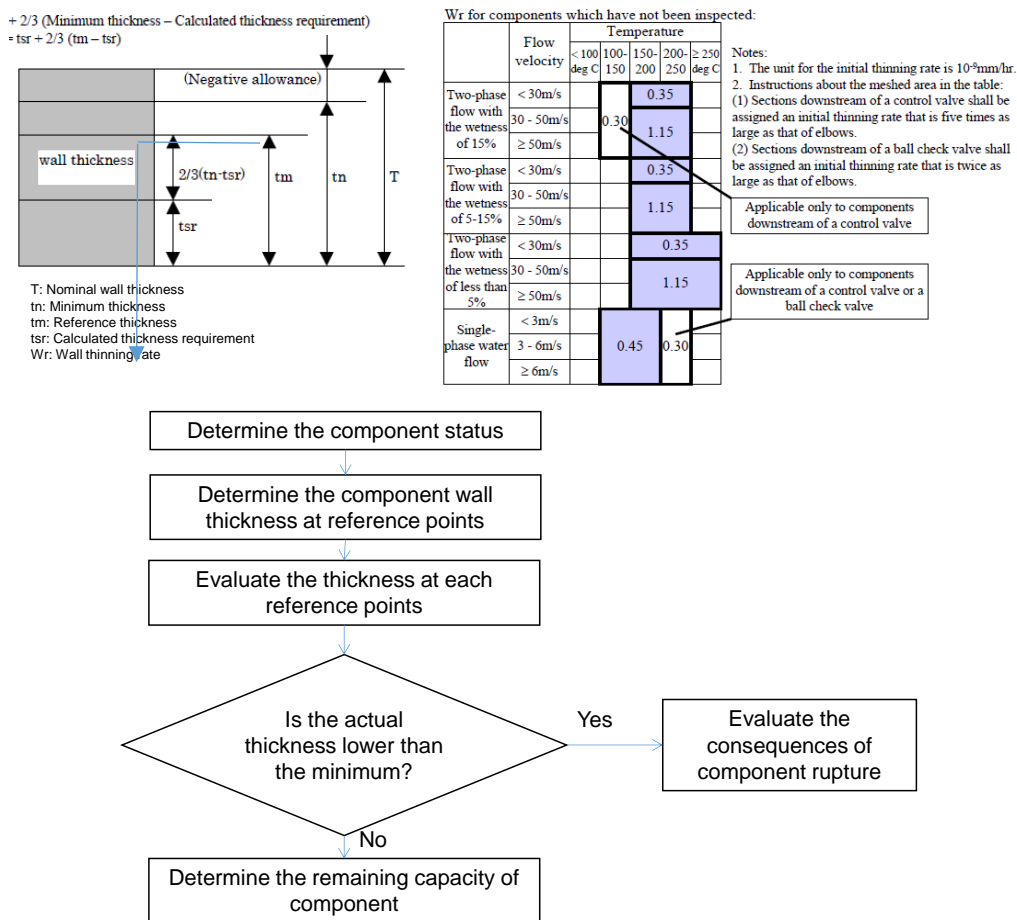


Figure 19: Schematic diagram for thinning investigation. In the top right table are summarised some experimental based value of the wearing thinning rate for different primary fluid conditions to take into account for analysis [33]

In monitoring the progression of the thinning, the electrical analogue may be used to quantify and predict the progression of the degradation. Since the temperature is the potential, or driving, function for the heat flow and the thermal resistance is dependent on the thermal conductivity, thickness of material and area, the thickness reduction, caused by the aging, can be determined based on the temperature gradient across the wall thickness [23].

Consequently, it will be possible to verify the structural capacity of the pipe, according to ASME III sect. NB-3232 [24] for its current thickness value. The remaining pipe service life is so dependent on the minimum thickness requirement and thinning rate.

In doing that, the heat inverse problem, allowing to reconstruct the temperature gradient based on the external temperature of the pipe, plays an important role as well as for thinning

investigation purposes, the knowledge of the annual rate of erosion/corrosion of the pipe (data obtained from material specifications).

### **5.1 Ageing analysis: the pipe thinning**

Large and long-life passive structure and components, such as pressure vessels, concrete structures, and pipe, are the most critical to assess in terms of safety and performance, this assessment is made even more difficult due to the lack of (in-depth) knowledge of aging phenomena and mechanisms. Therefore, to deal with the gap that characterizes the design of the actual SSCs of the existing plants, a design verification that considers the most demanding aspects of aging, in form of basic assumptions and/or input data, must be made.

In this study, both straight and bent part of a primary pipe are analysed; the pipe is indeed one of the most important plant subsystems that may be affected significantly by ageing phenomena.

Primary pipe shall be designed for the most severe condition of internal pressure and temperature allowed, and transient loadings. The nominal minimum thickness of a pipe wall [24], required for design pressure and for temperature not exceeding those for the various materials, is:

$$t_m = \frac{pD_0}{2(SE+Py)} + A$$

where  $t_m$  is the minimum thickness,  $p$  is the internal design pressure,  $D_0$  the outside diameter of pipe.  $SE$  is the maximum allowable stress in material at the design temperature,  $y$  is a numerical coefficient and  $A$  is the additional thickness to be consistent with the expected life of the pipe.

As aforementioned, based on the knowledge of the temperature gradient across the pipe wall it could be possible to determine the actual thickness value, and verify the bearing capacity of the pipe itself for LTO condition. The methodology to investigate the pipeline thermo-mechanical performance is consisting of:

1. reconstruction of temperature profile by inverse technique;
2. determination of all thermal and mechanical loadings;
3. identification of aging phenomena affecting the pipe;
4. thermo-mechanical analysis.

Thinning, which may ultimately cause perforation of the pipe wall if allowed to continue indefinitely, and the thermal degradation due to the operating conditions are considered. The former occurs throughout the affected region, rather than in a localized area as in the case of pitting or cracking, and is proportional to temperature, material, flow velocity, etc. The latter depends on the time and temperature of exposure, together with the material type and its chemical composition. The wall-thinning rates and the time-temperature dependent material property were considered [25].

The stresses to calculate ( $\sigma_r$ ,  $\sigma_\theta$  and  $\sigma_z$ ) for verification of load bearing capacity, for both steady and transient temperature distributions, are dependent on the mechanical and thermal loads and are expressed in cylindrical coordinate system as:

$$\sigma_r = \frac{E}{(1-\nu)} \left\{ -\frac{1}{r^2} \int_{r_i}^r \alpha T r dr + \frac{r^2 - r_i^2}{r^2(r_o^2 - r_i^2)} \int_{r_i}^{r_o} \alpha T r dr \right\} + \frac{(p_i r_i^2 - p_o r_o^2)}{r_i^2 - r_o^2} - \frac{1}{r^2} \frac{(p_i - p_o) r_o^2 r_i^2}{r^2(r_o^2 - r_i^2)}$$

$$\sigma_\theta = \frac{E}{(1-\nu)} \left\{ \frac{1}{r^2} \int_{r_i}^r \alpha T r dr + \frac{r^2 + r_i^2}{r^2(r_o^2 - r_i^2)} \int_{r_i}^{r_o} \alpha T r dr - \alpha T \right\} + \frac{p_i r_i^2 - p_o r_o^2}{r_o^2 - r_i^2} + \frac{(p_i - p_o) r_o^2 r_i^2}{r^2(r_o^2 - r_i^2)}$$

$$\sigma_z = \frac{E}{(1-\nu)} \left\{ \frac{2\nu}{(r_o^2 - r_i^2)} \int_{r_i}^{r_o} \alpha T r dr - \alpha T \right\}$$

where E is the Young's modulus,  $\alpha$  is the linear expansion coefficient,  $\nu$  is the Poisson's ratio, and r is the radial direction along which heat flows.  $r_i$  and  $r_o$  are the inner and outer radius of pipe, respectively, and T is the temperature.

The stress  $\sigma_z$  is independent from the pressure. From the above equations, it is easy to understand that, for an adequate evaluation of the pipe performance, it is necessary to determine the temperature.

### 5.1.1 Analysis of an aged straight pipe

The wall thinning is the consequence of the dissolution of the normally protective oxide layer from the surfaces of carbon and low alloy steel pipe. The wear rate depends on several parameters, some of the most important including the temperature and the hydrodynamics. Under single-phase conditions thinning was experienced in the temperature range from 80 to 230 °C, whereas between 140 and 260 °C under two-phase flow conditions.

When thinning mechanisms occur at local areas of pipe components, as shown in Yun et al. 2020 [26], degradation can cause eventually leaks or ruptures in the pressure boundary of NPPs. Reliable analyses to support inspection strategy become thus very important to prevent pipe rupture.

In this section, FE analyses of Gen II PWR pipe of about 78 cm diameter and about 5 cm thickness are presented in order to verify if the thinning is capable of jeopardizing the integrity of the primary system (Figure 20). The results from the CVM as well as the loads from/representative of the nominal operation were inputted to FE model (external coupling between MARC and Matlab codes). The model boundary conditions were the vertical supports at the edge and at intermediate pipe length; the initial conditions were the temperature and the internal pressure (14 MPa).

Material properties were assumed temperature dependent. A thermal expansion coefficient varying with the temperature was also imposed as well as the Von Mises criterion to measure the stress level to be used to calculate the failure probability. Several thinning rates, e.g. from 0.5 to 1.5 mm/yr, as caused mainly by flow acceleration corrosion, were considered for the thermo-mechanical analyses.

Band method is used to calculate wear rate of the pipe [27]. In addition, both homogeneous and heterogeneous thinning was analyzed. The effect of general pipe layout was not investigated.

It should be emphasized that thinning is not, in general, a mechanism that affects the internal surface of the pipe uniformly, as evidenced by the EPRI study [28] and by Yun et al. 2016 [29], due to the liquid droplet impingement erosion, cavitation etc. Accordingly, it becomes more difficult to identify in time before it can cause / trigger an incidental scenario. For these reasons, the simulations carried out have considered both the ideal-theoretical case of homogeneous thinning of the thickness along the whole pipe and the case of thinning localized along one generatrix or only in a part of the pipe.

The remaining service life of pipe (termed SOL in [27]) may be also calculated based on the knowledge of its minimum thickness ( $t_{min}$ ), minimum thickness requirement ( $t_{sr}$ ) and thinning rate ( $W_r$ ) and age (e.g.  $t_0+20$  yr,  $t_0+30$  yr;  $t_0+40$  yr, where  $t_0$  is the beginning of life) [30].

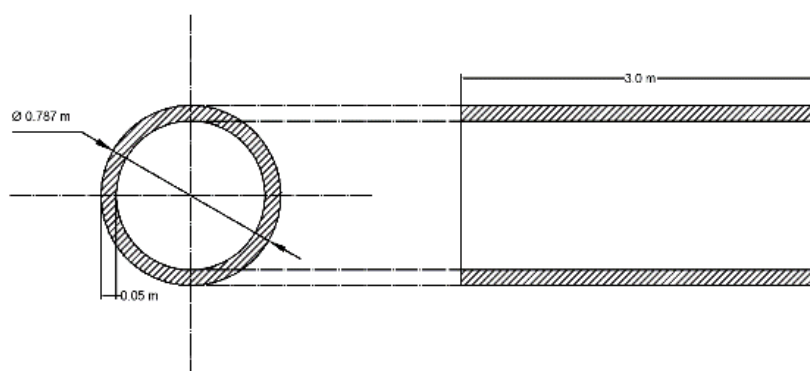


Figure 20: Schematic cross-section of a straight pipe. The geometry was reproduced exactly in the FE model

### 5.1.2 Straight pipe analysis results

In what follows the results obtained from the performed transient thermo-mechanical (numerical) analyses are presented.

The results show that LTO of the pipe, beyond 30 years of operation, is still possible if the annual corrosion rate is kept lower than 0.7 mm/yr (Table 6). Moreover, as  $W_r$  decreases the life of pipe increases (green boxes in Table 6). It can also be observed that the residual life ( $L_r$ ) of the pipe is dependent on the degradation of the material properties: assuming the same  $W_r$ , e.g. equal to 0.5 mm/yr, and for 20% reduction of the steel yielding strength the useful residual life passes from approximately 15.7 yr to about 1.5 yr (Table 7). Moreover, the red boxes indicate that the component should be replaced to not impair the safety of plant operation.

Table 6: Residual pipe wall thickness allowing the extension of life

Plant Life [y]	Residual pipe thickness ( $t_{nom} - W_r$ ) [cm]			
	$W_r= 1.5$	$W_r= 1.15$	$W_r= 0.7$	$W_r= 0.5$
10	3.5	3.85	4.3	4.5
20	2	2.7	3,6	4
30	0.5	1.55	2.9	3.5
40	-	0.4	2.2	3
50	-	-	1.5	2.5
60	-	-	0.8	2

Table 7: Residual life ( $L_r$ ) beyond 30 years operation vs structural strength decrease

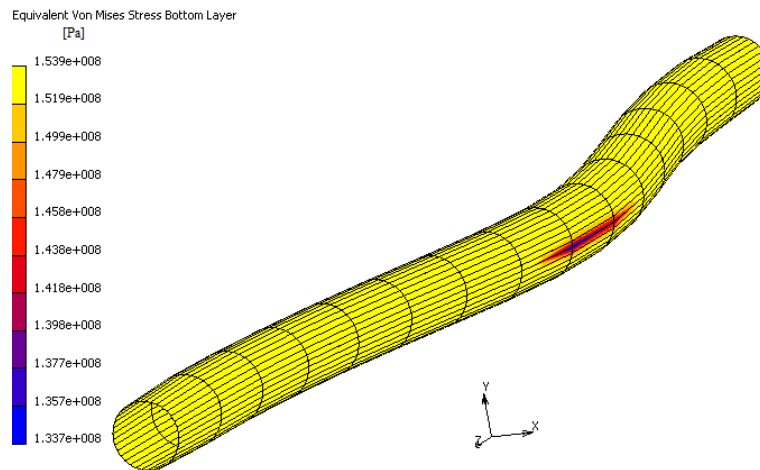
Residual Life [y]				Yielding Strength [% nominal value]
$W_r=0.5$	$W_r=0.7$	$W_r=1.15$	$W_r=1.5$	
15.72	2.66	-	-	100
12.76	0.55	-	-	95
9.46	-	-	-	90
5.76	-	-	-	85
1.57	-	-		80

Analysing the results of Table 6 against the ASME criterion of “87.5% of nominal wall thickness” (used to determine whether continued operation is acceptable or if a repair or replacement has to be implemented prior to return to service) we can say that for  $W_r \ll 0.5$  mm/yr the component thickness may be considered adequate for the service. Whether the residual wall thickness is below  $0.875 t_{nom}$  ( $< 3.925$  cm) a further (re)evaluation is required. Furthermore, the thermal gradient ( $\Delta T$ ) will increase in proportion to the ratio between the nominal thickness and the residual thickness of the pipe, in the case of normal operation hypothesis and for unchanged thermal conductivity, therefore, it is possible to control the pipe performance by monitoring the external temperature ( $T_{out} = T_{int} + \Delta T$ ).

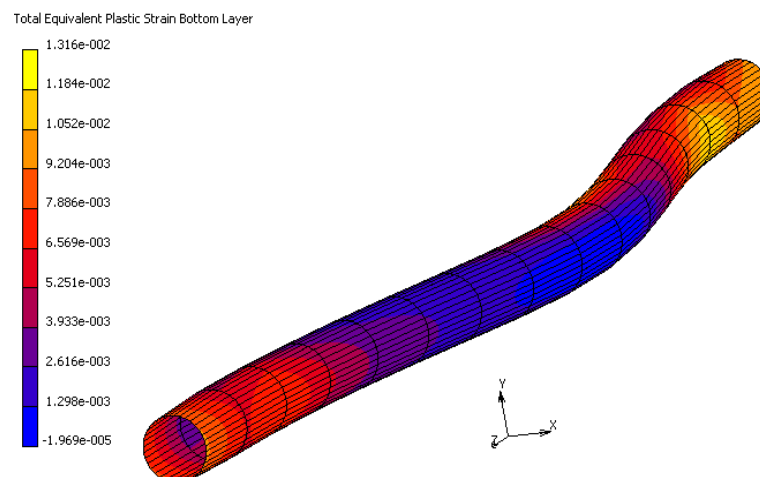
The generalised thinning involves throughout the surface of steel when a slow and uniformly distributed loss of material appears. However, this general degradation mechanism is not responsible of any appreciable localized deformation and/or damage.

In Figure 21 are shown the equivalent von Mises stress and the resulting plastic deformation for localised thickness reduction: different deformations appear at the pipe surface caused by the localized thickness reduction up to 0.8 cm.

They are mainly located in the areas of the maximum deflection where thinning degradation is worse (and could be even more because of the liquid impingement).



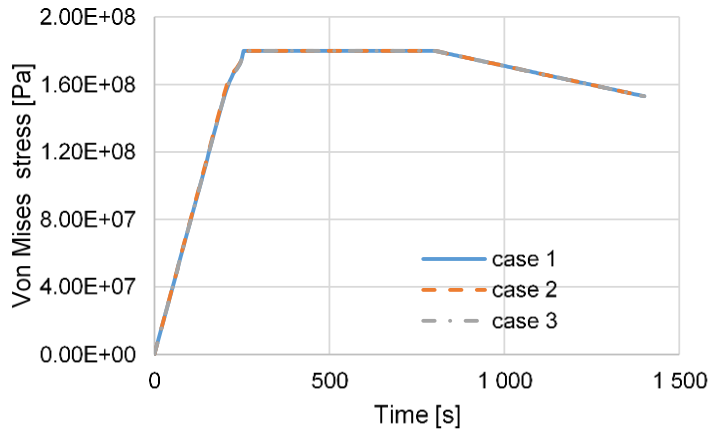
(a)



(b)

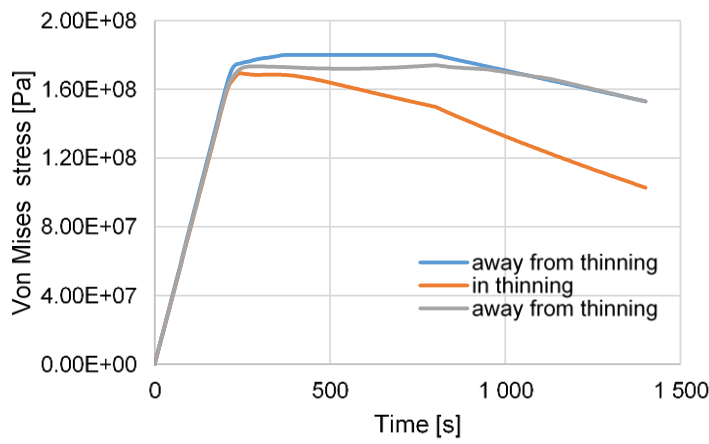
Figure 21 a, b: Equivalent Von Mises stress(a) (at the bottom layer) and the resulting plastic deformation (b) for localised and heterogeneous thickness reduction. The nominal pipe thickness, 30 yr aged, is  $t_{nom}=1.55$  cm (Table 6); while the section with localized thinning has  $t_{reduced}= 0.8$  cm

By comparing the stress plots provided in



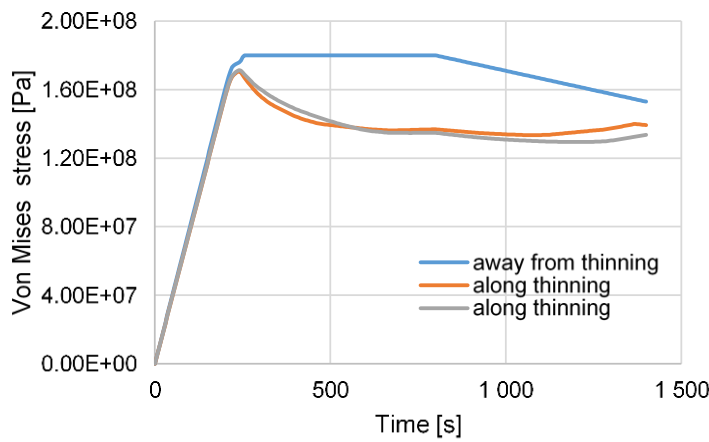
Case 1:  $t = 3.5$  cm  
Case 2:  $t = 2.9$  cm  
Case 3:  $t = 1.55$  cm

a)



Case 4:  $t = 1.55$  cm

b)



Case 5:  $t = 1.55$  cm

c)

Figure

22

and

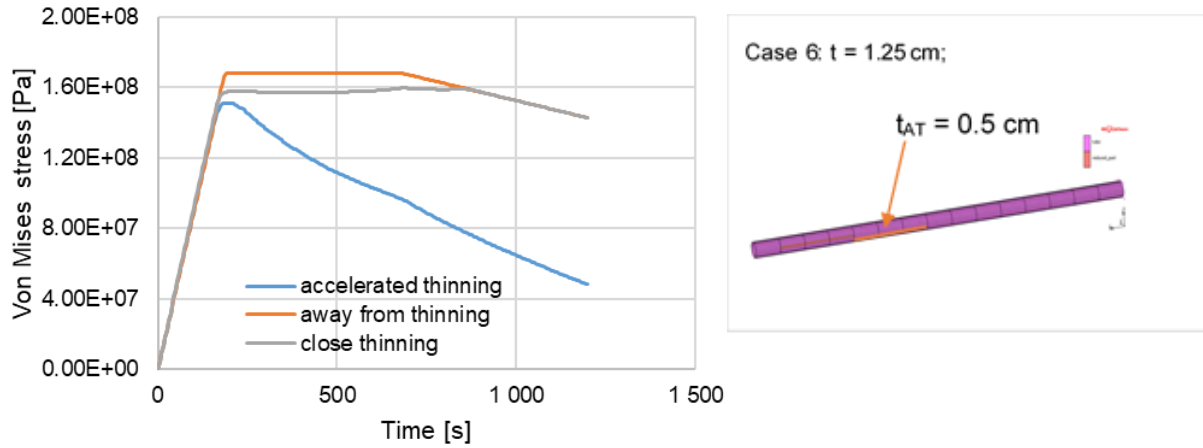
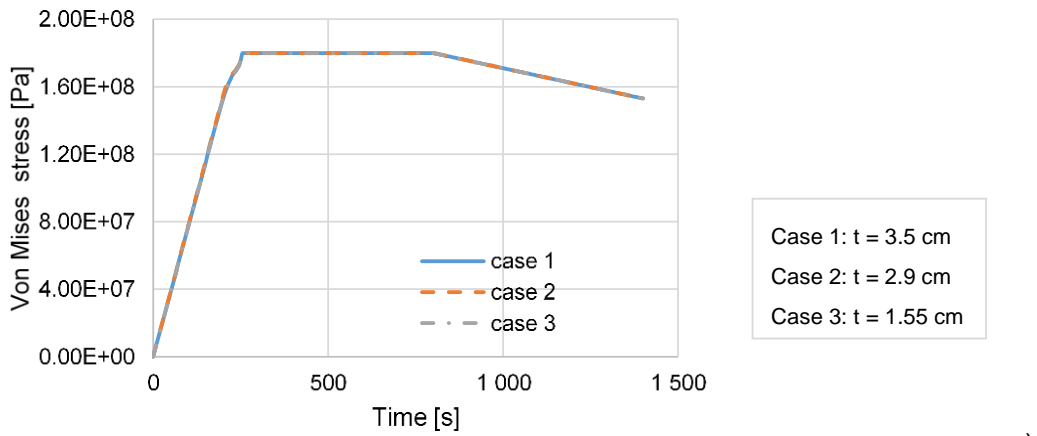
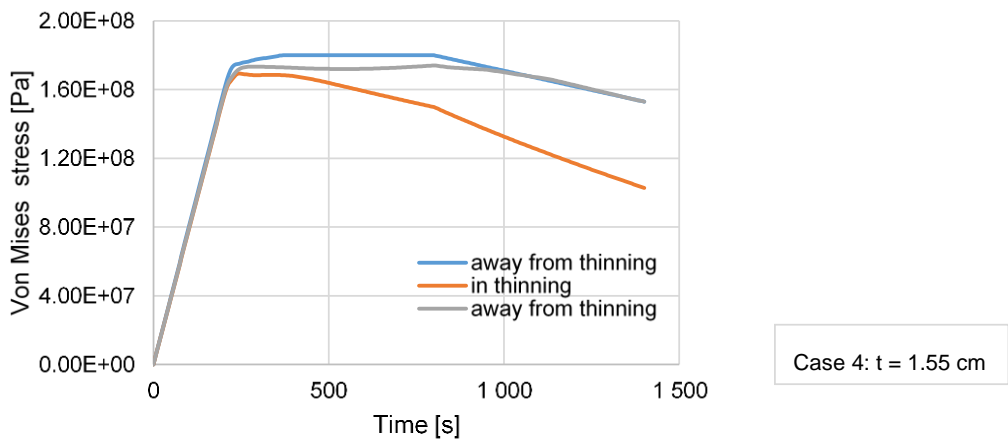


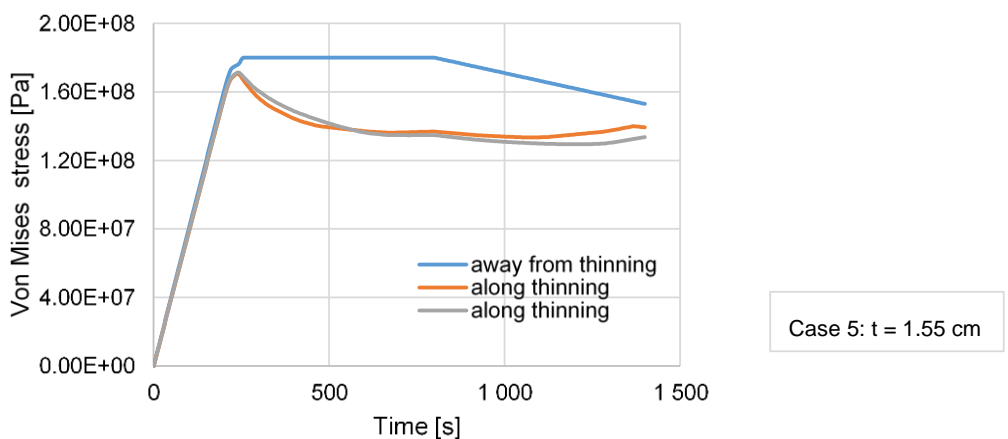
Figure 23, and taking into account that the pipe is subjected to the same Class I load combinations, it possible to say that the structural integrity is assured even when heterogeneous thickness reduction, caused by accelerated ageing and premature degradation, occurs.



a)



b)



c)

Figure 22 a, b, c: Equivalent Von Mises stress (at the bottom layer) for pipe subjected to homogenous thinning (a) and thinning localized along a generatrix (b) and in a part of pipe (c). In these simulations, actual yielding strength is considered

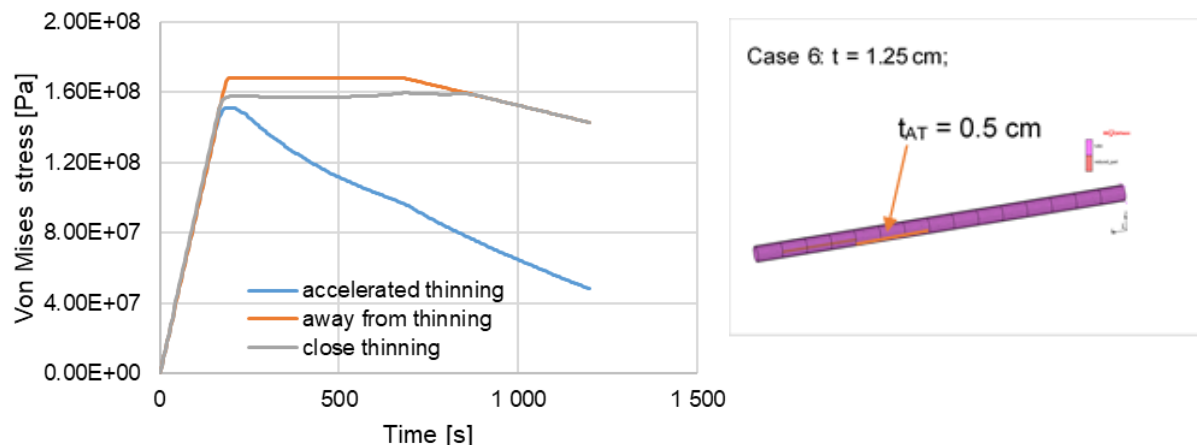


Figure 23: Equivalent Von Mises stress (at the bottom layer) of pipe subjected to heterogeneous and accelerated thinning-AT- (orange colored).

### 5.1.3 Analysis of an aged bent pipe

The behavior of an elbow pipe along its longitudinal direction is also studied (complex geometry). The loading condition is the same considered in section 5.1.1.

Thinning, in this case, is expected to be more severe because the geometry varies drastically or is more complex: change in direction of the flow makes item susceptible to both erosion and corrosion damage. The synergy between erosion and corrosion further aggravates the internal surface area damage. In this case, the impact of creep was also taken into account.

For FE simulations, a 3D model representing a primary bent pipe, made of AISI 304, was set up and implemented. Figure 24 and

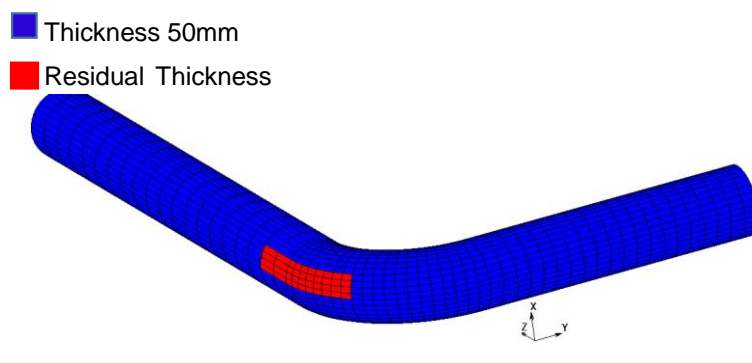


Figure 25 show respectively the cross section and the geometry of the bent pipe and the 3D meshed model. In addition, in the model, the part of the elbow pipe suffering thickness reduction is red colored.

The model is completely symmetrical about Z-Y plane without consideration neither of inlet/exhaust joint pipe nor of the flowing coolant.

The FE analysis aims to study the behaviour of the item for 700 hrs beyond 30 years of service operation.

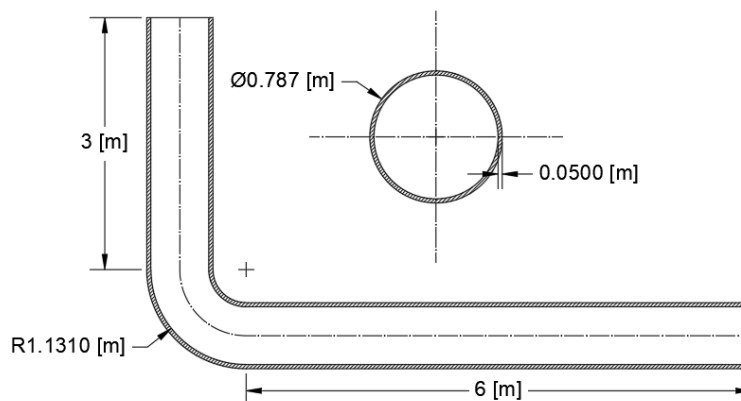


Figure 24: Cross-section of the bent pipe. Geometrical dimensions are in [m]

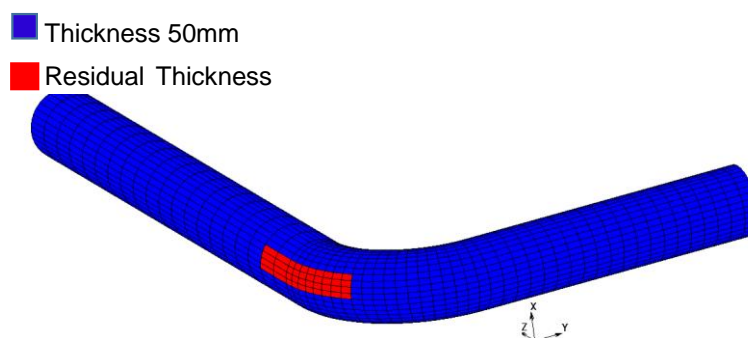


Figure 25: 3D FE model of the bent pipe

In the numerical assessment, we assumed thinning rates ( $W_r$ ) of the elbow e.g., equal to 0.5 mm/yr and 0.7 mm/yr, and 20% reduction of the nominal steel material properties [31][32]. Concerning corrosion/erosion phenomena, thinning rate are determined based on the lesson learned from Davis Besse NPP (USA), Japanese Mihama Unit 3 NPP accident [33], the study performed by Oh et al. [34] and the database [32].

The RPV vessel closure head inspections of Davis Besse plant revealed a large cavity in the 15.24 cm thick low-alloy carbon steel RPV head material. This cavity was about 16.76 cm long and 10.16 to 12.70 cm at the widest point extending down to the 0.635 cm thick type 308 stainless steel cladding.

The 2004 accident in the Mihama Unit 3 NPP highlighted that the turbine return pipe after 27 years in service reduced its thickness to about 1.4 mm, corresponding to 86% loss in thickness and too harsh pressure-temperature conditions to sustain for the remaining pipe material.

The reduction of nominal steel material properties, procedures, correlations and data for forecasting changes in mechanical properties of the stainless steel items are provided in [35]. Material data are calculated considering a thermal aging (280-330° C for 58,000 hrs) during service in light water reactors [36].

For FE analysis, after 30 years of nominal operation, the thickness of wall is assumed 35 mm and 29 mm for thinning rate of 0.5mm/yr and 0.7mm/yr respectively. These values are used as boundary conditions for the thermo-structural analysis. The reduction of pipe thickness is not updated as transient progresses. To this end, the slight overestimation of residual life associated to the thickness variation of about 0.55 mm, calculated assuming  $W_r = 0.7$  mm/yr for 700 hrs, does not affect the overall results. The bent pipe is fully constrained at the two ends, i.e., clamps allowing the only expansion in Z and Y directions, respectively for the long and short pipe run. With reference to the study [37], an inner pressure of 14 MPa and a constant temperature of 300° C are set-up for the entire transient of 700 hrs.

Material properties of the numerical model are assumed temperature dependent, according with Table 8, particularly those at 300° C. The AISI-304 properties are extracted from a materials database available in [38], collecting over 450,000 metals, polymers, ceramics, and composites material properties experimentally obtained in compliance with international regulations (e.g., ASME, ASTM). These validated data are hence implemented in ageing model. Von Mises criterion is chosen to measure the stress level.

Table 8: Thermo-mechanical properties of AISI304 [32]

Temperature (°C)	Density (kg/m <sup>3</sup> )	Specific heat (J/kg °K)	Conductivity (W/m °K)	Thermal expansion (x10 <sup>-5</sup> °K <sup>-1</sup> )	Yield stress (MPa)	Young's modulus (GPa)	Poisson's ratio (-)
-200	7900	157	8.4	1.22	412	181	0.294
-100	7900	380	12.6	1.43	319	181	0.294
0	7900	462	14.6	1.7	265	199	0.294
100	7880	496	15.1	1.74	218	193	0.295
200	7830	512	16.1	1.8	186	185	0.301
300	7790	525	17.9	1.86	170	176	0.31
400	7750	540	18	1.91	155	167	0.318
600	7660	577	20.8	1.96	149	159	0.326

A coupled thermo-mechanical viscoplastic analysis was performed in order to verify the structural integrity of the item. No hardening is considered.

Multiple domains and independent or dependent variables representing various physical systems are included in the concept of coupled systems. When there are several domains involved, the solution for both domains is obtained at the same time.

Coupled systems can be divided into two categories:

- Interface variables coupling: in this set of problems, a coupling happens via the domain interfaces. Domains can be physically different (e.g., fluid-solid interaction) or physically the same but with distinct discretization (e.g., mesh partition with explicit/implicit processes in different domains).
- Field variables coupling: the domain may be the same or different. Coupling operates by differential equations that describe various physical phenomena, e.g., coupled thermo-mechanical problems.

Coupling between thermal and mechanical problems takes place by means of temperature-dependent material properties in the mechanical (stress) problem and internal heat generation in the mechanical problem induced by plastic work, which is used as input for the problem of heat transfer. Temperature distribution and displacement are obtained. The effect of changes in the temperature distribution contributes to the deformation of the body through thermal strains and influences the material properties. There are two main reasons for the coupling. First, the coupling takes place when the deformation causes a shift in the related heat transfer problem, while the second cause of coupling is heat generated due to inelastic deformation.

The coupling between the heat transfer problem and the mechanical problem is so due to the temperature-dependent mechanical properties and the internal heat generated. Thermo-structural analysis is a coupling type of analysis where the two physics passes are performed one after the other. The Kirchhoff constraints will tie the temperature of the bound node to the temperature of the projection point on its corresponding patch during the heat transfer pass of an increment.

In the viscoplastic model, plastic element is inactive for stress smaller than the yielding stress of the material [37]. As the transient progresses, the properties of AISI304 degrade and the implemented creep model describes the primary and secondary stage.

The ratio thickness/diameter is less than 0.1, therefore the model is implemented with doubly curved thin shell elements. This selected element is a four-node, thin-shell type with global displacements and rotations as degrees of freedom. Bilinear interpolation is used for the coordinates, displacements, and the rotations. The element is defined geometrically by the (x, y, z) coordinates of the four corner nodes. Due to the bilinear interpolation, the surface forms

a hyperbolic paraboloid, which is allowed to degenerate to a plate. The stress output is given in local orthogonal surface directions,  $V_1$ ,  $V_2$ , and  $V_3$ .

The shell elements are numerically integrated through the thickness and the membrane strains are obtained from the displacement field. The number of layers through the thickness in the implemented model are eleven. The layer numbering convention is that the first layer is on the positive normal side of the shell, and the last layer is on the negative normal side.

The element normal is determined through the coordinates of the nodal position as well as the element's connectivity. Simpson's law is used to carry out the field variable integration for problems involving homogeneous materials.

**5.1.4 Bent pipe analysis results**

The performed coupled thermo-structural-viscoplastic simulations focused on the study of combined effect of creep, thinning and aging for bent pipe, beyond 30 years of nominal operation. According to the study [31], five different cases have been considered:

- Case 1: no creep, thinning, and material properties reduction. This is the reference case.
- Case 2: 0.5 mm/yr with 10% of the steel properties reduction;
- Case 3: 0.5 mm/yr with 20% of the steel properties reduction;
- Case 4: 0.7 mm/yr with 10% of the steel properties reduction;
- Case 5: 0.7 mm/yr with 20% of the steel properties reduction.

The worst cases are represented by the Case 3 and the Case 5 for different  $W_r$ .

$W_r$  of 0.5 mm/yr and 80% of steel properties should guarantee the structural integrity for 1.57 years beyond the 30 years of plant nominal operation, if  $W_r$  increases (e.g. up to 0.7 mm/yr) the structural integrity of item is no more guaranteed, as shown in Table 9. This means that the item must be replaced.

Table 9: Residual life ( $L_r$ ) beyond 30 years operation vs. AISI304 properties reduction [31]

Residual Life [y]		AISI304 Properties [% nominal value]
$W_r=0.5$ mm/yr	$W_r=0.7$ mm/yr	
15.72	2.66	100
9.46	-	90
1.57	-	80

The results show that the most stressed part of pipeline is the outer elbow section considering a  $W_r$  of 0.7mm/yr, especially where the thickness is reduced.

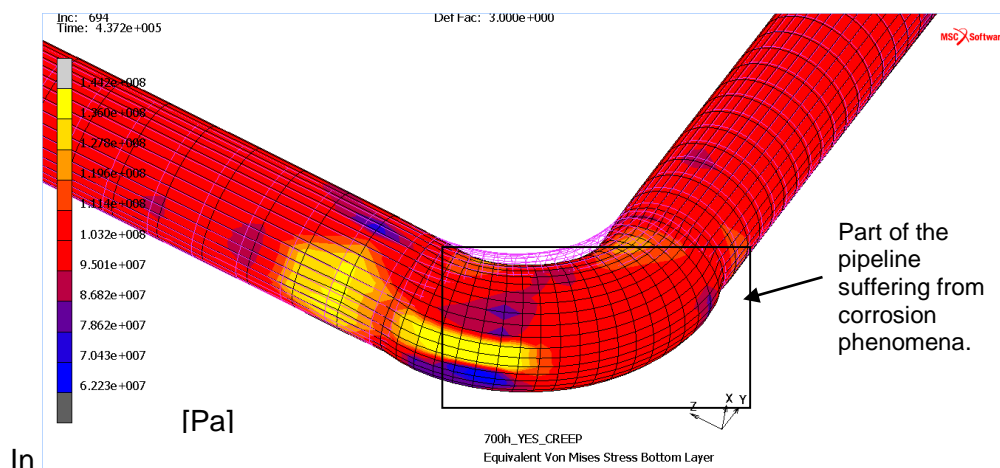


Figure 26, Figure 27, and Figure 28, are represented the top and bottom layers of equivalent Von Mises stress and the total equivalent creep strain for the worst Case 5.

Flexural deformation appears and becomes even worse when thinning increases. Eccentric bending may appear and determine cross section ovalization with or without bulging at the pipe outer surface. And it may be responsible for buckling of pipeline. Moreover, by analyzing the stress contour plot, it emerges that the flexural effects are not localized but extend also in the straight part.

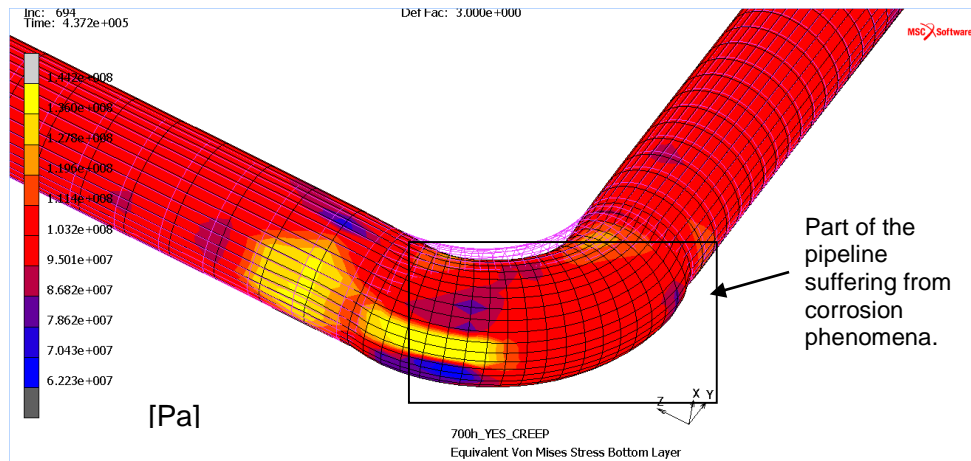


Figure 26: Equivalent Von Mises stress bottom layer – Case 5

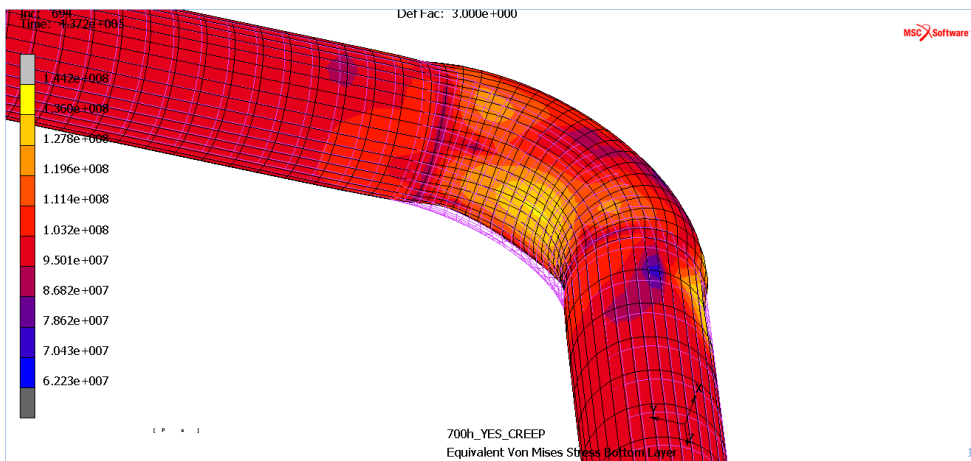


Figure 27: Equivalent Von Mises stress bottom layer – Case 5

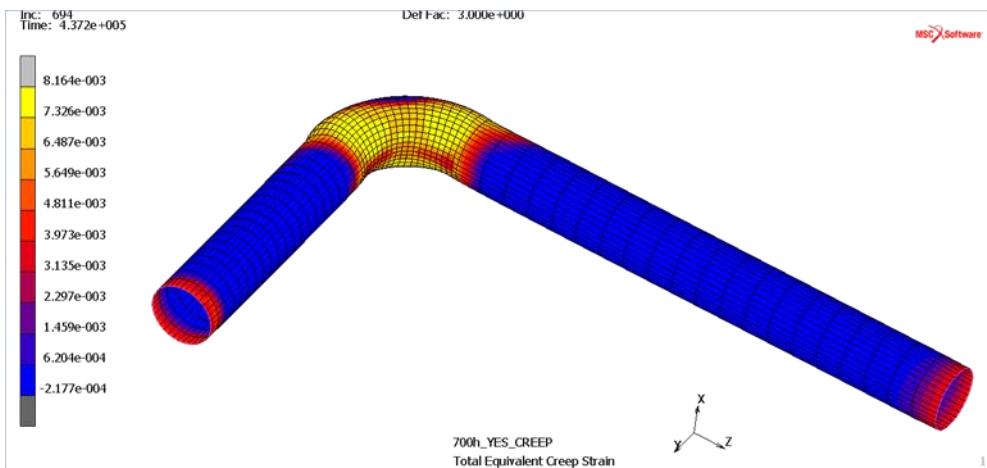


Figure 28: Total equivalent creep strain – Case 5

The results confirm the provision for a linear pipe in the study [31]; the structure reaches the plastic limit load after 121.45 hours of nominal operation as shown in

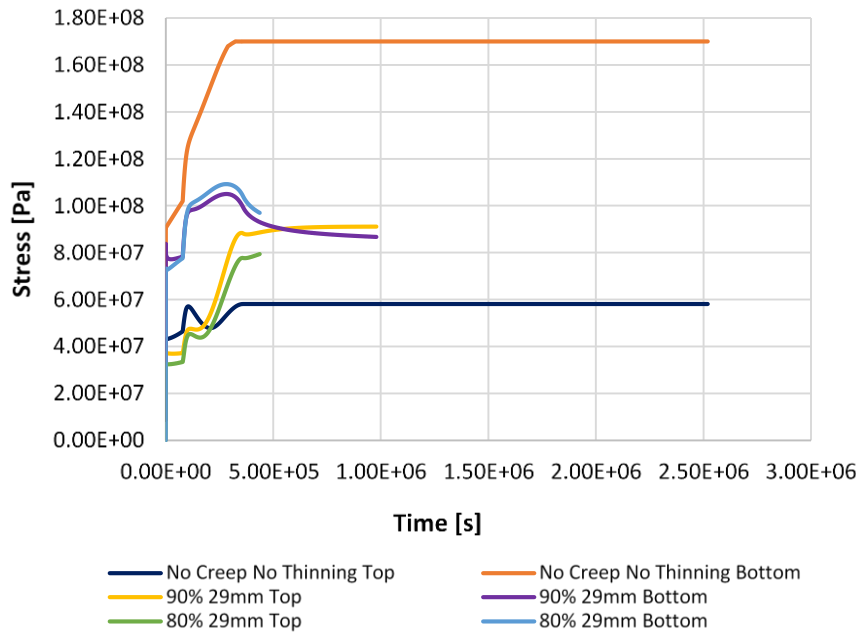


Figure 29, Figure 30 and Figure 31. Instead, in the case 3, the item does not reach the plastic limit load and the thermo-mechanical analysis is completed as shown in Figure 32; the component may be considered adequate for the service.

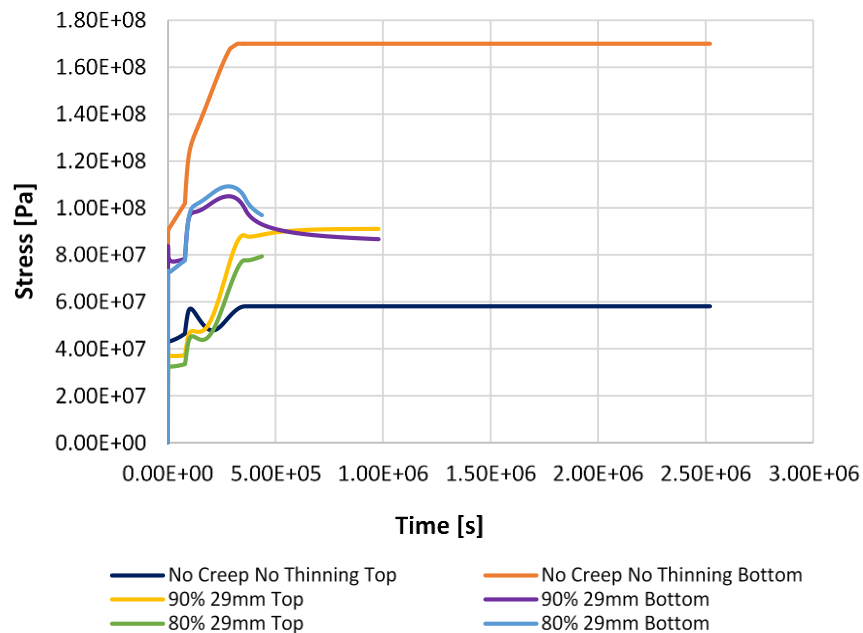


Figure 29: Top and bottom equivalent layers of equivalent von Mises stress away from thinning – Case 1 (reference); Case 4; Case 5

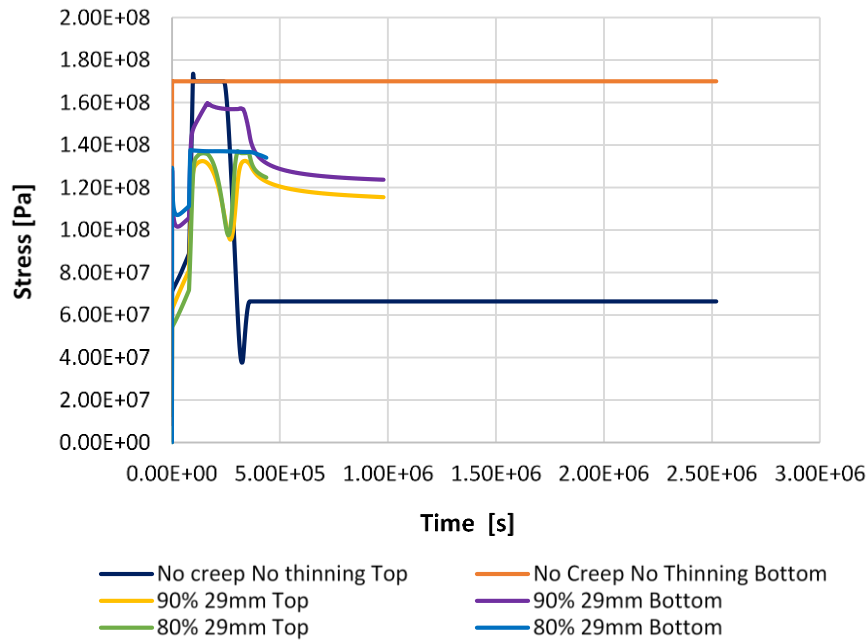


Figure 30: Top and bottom layers of equivalent von Mises stress in thinning - Case 1 (reference); Case 4; Case 5

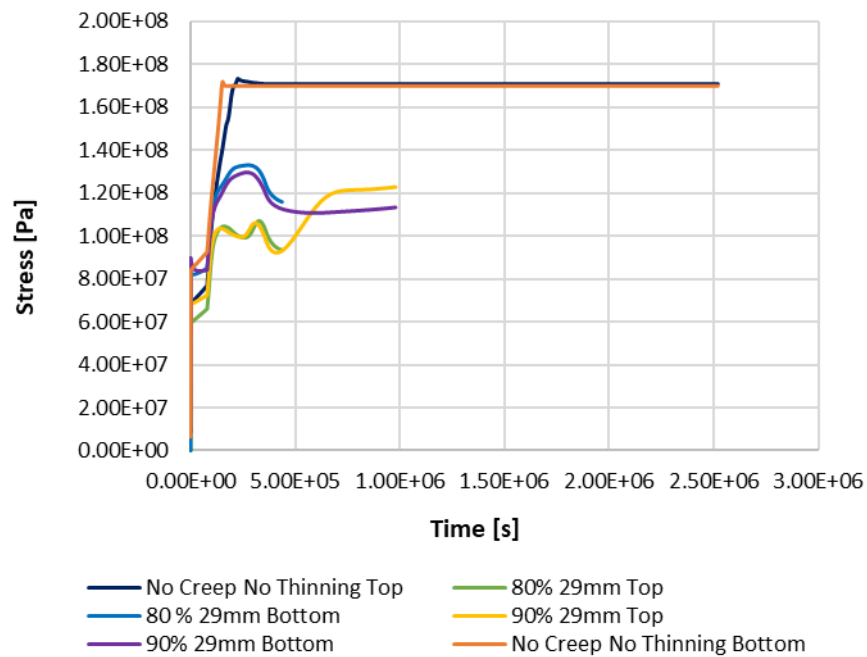


Figure 31: Top and bottom layers of equivalent von Mises stress in thinning - Case 1 (reference); Case 4; Case 5

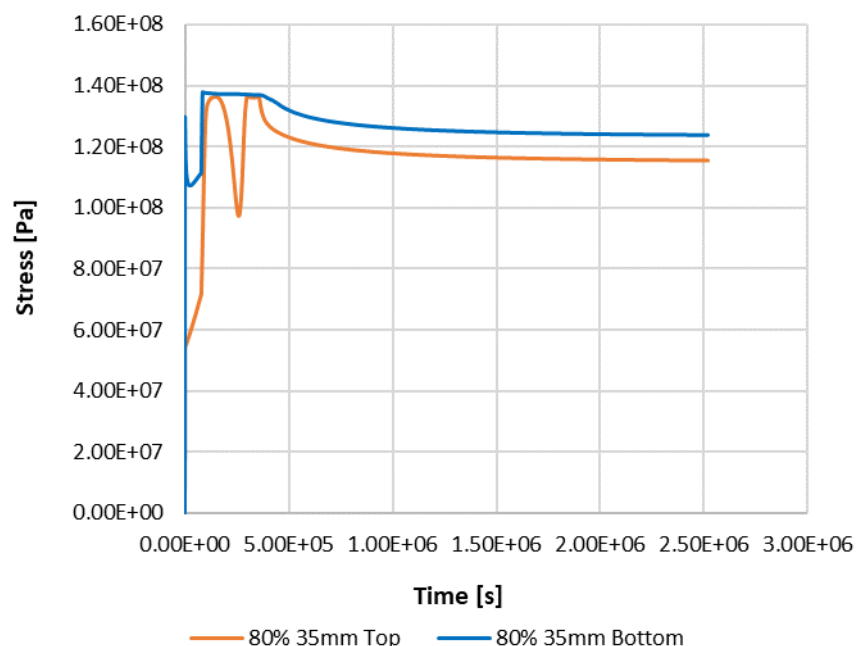


Figure 32: Top and bottom layers of equivalent von Mises stress in thinning – Case 3

The thinning, aging and creep effects, as observed, strongly reduce the strength capacity, and their jeopardizing effects become even more relevant as long-term material corrosion, aging and creep progress. This aspect is of fundamental importance in view of the life extension of the existing NPPs and for planning efficient plant life management.

The above shown results indicated that in the Case 2 and Case 3, the bent pipe even aged retained the required safety margin demonstrating that the component is adequate for continuing the service operation.

The simultaneous effects of creep, thinning and reduction of structural capacity due to aging seemed capable to reduce the structural integrity of the component even for a small variation of the mechanical properties if  $W_r$  is equal to or greater than 0.7.

In the Case 4 with 90% of nominal properties of AISI304, the component fails after about 272 hrs., while in the Case 5 (the worst) it fails after about 121.45 hrs.

In the Case 5 with only a reduction of 10% more of steel's thermomechanical properties the item fails in half of time (about 55%) than in the Case 4.

The localized thinning, aging and creep effects, as observed, strongly reduce the strength capacity, and their consequences become even more relevant as component life progresses [39]. The role of creep becomes marginal compared to thinning and other aging phenomena even after 30 years operation because the given operating temperature (far lower than  $0.4T_m$ ).

The flow pattern in an elbow is subjected to great changes in direction and velocity, leading to significant difference in corrosion behavior at different locations (inhomogeneous thinning).

## 5.2 Main conclusions

By coupling the inverse space marching method to verify the capability of a PWR primary, aged pipe, the thermo-mechanical analysis demonstrates that the pipe retains the required safety margin for long term operation.

The thermal analogue seems to be a suitable method to control the progression of thinning by controlling and reconstructing the internal temperature of the pipe.

The FEM analyses allowed to determine the pipe capacity of guaranteeing the operating conditions for different rate and type (localized or generalized) of thinning.

In summary, the carried-out analyses have highlighted:

- For  $W_r=0.5$  mm/y and strength reduction (80% nominal value), the useful life of the component decreases approximately of 20%.
- The thermal gradient increases in proportion to the ratio between the nominal thickness and the residual thickness of the pipe. Consequently, it is possible to control the pipe degradation and performance by monitoring the external pipe surface temperature.
- Slow and uniformly generalised thinning involving throughout the surface of steel pipe is not responsible of any appreciable localized deformation and/or damage. The opposite happens for localised thinning, particularly for the heterogeneous one, that is characterised by flexural effects that become more and more marked as time passes and thinning progresses. Bending deformation modes appears along the length of pipe generatrix (see Figure 21 b).
- Even when the PWR operating conditions (e.g. temperature, pressure, water chemistry) are outside the prescribed operating limits, if  $W_r$  is less than 0.5 mm/y, the pipe perforation could be avoided for another 30 years of normal operation (LTO of 60 years) in the absence of other factors that could further degrade the pipe performance.

Finally, it is worthy to remark that the thinning of steel pipe and related components is a continuous and almost irreversible process, for this reason, timely feedbacks coming from experience and assessment (implementation of effective management programmes) are essential to prevent unacceptable ageing degradation that could jeopardize the plant integrity.

For the “aged” bent pipe, beyond 30 years of nominal operation, results highlight:

- In the Case 2 and Case 3, the pipe retains sufficient safety margin for LTO: pipe is so adequate for service operation.
- For case 4 and case 5 the component fails at 272 hrs. and 121.45 hrs. respectively demonstrating that aging and high thinning rate (0.7 mm/yr) threat the pipe capacity (limit state is reached).
- Flexural deformation is not localized but extends also in the straight part of pipe. It becomes even worse as thinning increases.
- Eccentric bending determines the ovalization of the pipe cross section (buckling phenomenon).
- The role of creep becomes marginal compared to thinning and aging even after 30 years operation because the given operating temperature (far lower than  $0.4T_m$ ).
- Consequences of localized thinning, aging and creep become even more relevant as the lifetime of component progresses. The greater the materials' degradation, the lower the residual resistance capacity and the greater the risk for LTO.

## 6 Conclusions

A preliminary evaluation of the reliability of Gen III NPP components relevant for safety subjected to earthquake events and ageing was performed.

The results from the several different analyses confirmed that ageing (e.g., damaging phenomena, corrosion) of structural elements is likely to degrade the mechanical performance and impair the resistance capacity of these elements, minimizing in the better case the residual safety margin.

The impact of different stages of ageing on the seismic resistance structures, allowing to integrate the deterioration of response capacity in the fragility assessment, highlighted: acceleration amplifies of 4 times at the dome of the internal containment than the input ground motion. Accordingly higher is the equivalent Von Mises stress generated within the items cross-section. The greater the reduction in material strength caused by the ageing, the greater the reduction in the structural capacity and the larger the damage suffered by the concrete.

Moreover, the mean value of relative horizontal displacement of about 12 mm at e.g. SG elevation, suggests structural problems may arise for piping, anchorage/restraining systems and penetrations.

The results from the analyses carried out on the primary pipe (straight and bent part of it) show:

- For  $W_r=0.5$  mm/y and strength reduction (80% nominal value), the useful life of the pipe decreases approximately of 20%.
- Slow and uniformly generalised thinning involving throughout the surface of steel pipe is not responsible of any appreciable localized deformation and/or damage. The opposite happens for localised thinning, particularly for the heterogeneous one, that is characterised by flexural effects that become more and more marked as time passes and thinning progresses. Bending deformation modes appears along the length of pipe generatrix.
- Even when the operating conditions (e.g. temperature, pressure, water chemistry) are outside the prescribed operating limits, if  $W_r$  is less than 0.5 mm/y, the pipe perforation could be avoided for another 30 years of normal operation (LTO of 60 years) in the absence of other factors that could further degrade the pipe performance.
- The combined effects of different simultaneous mechanisms such as creep, thinning and reduction of structural capacity reduce the structural integrity, even for a small variation of the mechanical properties, if  $W_r$  is equal to or greater than 0.7.
- Flexural deformation extends becomes even worse as thinning increases. It is the eccentric bending that determines the ovalization of the pipe cross section and may trigger buckling phenomenon.

The FE model used demonstrated to be a suitable tool to account for cumulative effects by succession of events and ageing mechanisms; in this way the residual capacity as well as the residual life of SSCs can be determined.

Finally, it was demonstrated the importance of the numerical modelling as a predictive and flexible tool capable to evaluate the performance of the degraded component (or similar components in parallel lines) and ensure a safe operation of plant.

The data obtained may represent the input data for fragility assessment as indicated in task 2.3.

While this study presented the impact of different ageing mechanisms, such as damaging phenomena and corrosion, on the performance and seismic resistance of plant structures, it is expected to expand the numerical simulation approach to multi-hazard events in order to represent the reliability of NPP components and sub-systems. Additional developments will be necessary to go beyond this stage and include further material degradations (and their cumulative effects), e.g., erosion, embrittlement, stress relaxation etc., into the fragility assessment of NPP components.

## 7 References

- [1] International Energy Agency (2021), Net Zero by 2050 A Roadmap for the Global Energy Sector.
- [2] Nuclear Energy Agency (2021), Long-Term Operation of Nuclear Power Plants and Decarbonisation Strategies, NEA No. 7524
- [3] International Atomic Energy Agency, Specific Safety Requirements No. SSR 2/1 (Rev 1), Safety of Nuclear Power Plants: Design, IAEA, Vienna (2016).
- [4] International Atomic Energy Agency (2018), Ageing Management and Development of a Programme for Long Term Operation of Nuclear Power Plants, Specific Safety Guide No. SSG-48
- [5] IAEA. Handbook on ageing management for nuclear power plants, no. NP-T-3.24, 2017
- [6] IAEA. Assessment and management of ageing of major nuclear power plant components important to safety - Primary piping in PWRs. TECDOC-1361, 2003
- [7] <http://www.narsis.eu>
- [8] Y. Kitada et al., Models test on dynamic structure–structure interaction of nuclear power plant buildings, Nuclear Engineering and Design 192 (1999) 205–216.
- [9] Y. Zhao et al. (1996). Nonlinear 3-D dynamic time history analysis in the reracking modifications for a nuclear power plant”, Nuclear Engineering and Design 165,199-211.
- [10] R. Lo Frano, G. Forasassi, Preliminary evaluation of the reliability of Gen II or III reactors in BDBE conditions Proceedings of the 2012 20th ICONE20-POWER2012, July 30 - August 3, 2011, Anaheim, California, USA
- [11] American Concrete Institute, Code Requirements for Nuclear Safety-Related Concrete Structures, ACI Standard 349-01 and Commentary, 2001.
- [12] International Atomic Energy Agency, Deterministic safety analysis for nuclear power plants, IAEA Safety Standards Series No. SSG-2 (Rev. 1), 2019.
- [13] R. Lo Frano, G. Pugliese, and G. Forasassi (2010). Preliminary seismic analysis of an innovative near term reactor: Methodology and application, Nuclear Engineering and Design, vol. 240, issue 6, 1671-1678.
- [14] J. W. Baker (2011). Conditional Mean Spectrum: Tool for Ground-Motion Selection, J. Struct. Eng., 137(3), 322-331
- [15] International Atomic Energy Agency, Geotechnical aspects of site evaluation and foundations for nuclear power plants, Safety Standards Series No. NS-G-3.6, 2004
- [16] U.S. Nuclear Regulatory Commission (NRC), 2012. Rev. 3, Regulatory Guide 1.92. Combining Modal Response and Spatial Components in Seismic Response Analysis
- [17] H. Bachmanet et al., Vibration Problems in Structures, Birkhäuser Basel, 1995.
- [18] Electric Power Research Institute (EPRI), TR-106611-R1, Flow Accelerated Corrosion in Power Plants, 2002.
- [19] Y.H. Choi, S.C. Kang, Evaluation of Piping Integrity in Thinned Main Feedwater Pipes. Nucl. Eng. Technol., 32, 67–76, 2000.
- [20] R. B. Dooley, V.K. Chexal, Flow-accelerated corrosion of pressure vessels in fossil plants. Int. J. Press.Vessels Pip. 77, 85–90, 2000.
- [21] R. Lo Frano and G. Forasassi, Buckling of imperfect thin cylindrical shell under lateral pressure, Science and Technology of Nuclear Installations 2008,685805

- [22] R. Lo Frano and G. Forasassi, Experimental evidence of imperfection influence on the buckling of thin cylindrical shell under uniform external pressure, *Nuclear Engineering and Design*, 239(2),193-200, 2009
- [23] R. B. Hetnarski, M.R. Eslami. *Thermal stresses – Advanced Theory and Applications*. II Ed. Springer.
- [24] ASME III, Division 1 – subsection NB-3232, ASME, Boiler and Pressure Vessel Committee, 1980
- [25] M. Matsumura (2015), Wall thinning in carbon steel pipeline carrying pure water at high temperature, *Materials and Corrosion*, 66, No. 7, 688-694
- [26] H. Yun et al. Development of wall-thinning evaluation procedure for nuclear power plant piping - Part 2: Local wall-thinning estimation method, *Nuclear Engineering and Technology*, Vol. 52, Issue 9, 2119-2129, 2020
- [27] NEA/OECD, Flow Accelerated Corrosion (FAC) of Carbon Steel & Low Alloy Steel Piping in Commercial Nuclear Power Plants, NEA/CSNI/R(2014)6, June 2014
- [28] EPRI, Chug Position paper No.8, Determining Piping Wear Caused by Flow-Accelerated Corrosion from Single-Outage Inspection Data, 2006.
- [29] H. Yun, S.J. Moon, Y.J. Oh. Development of wall-thinning evaluation procedure for nuclear power plant piping - Part 1: Quantification of thickness measurement deviation, *Nuclear Engineering and Technology* 48 (No. 3) 820-830, 2016.
- [30] T.A. Netto, U.S. Ferraz, A. Botto. On the effect of corrosion defects on the collapse pressure of pipelines. *International Journal of Solids and Structures*, 44, Issues 22–23, 7597-7614, 2007.
- [31] S. A. Cancemi and R. L. F. Frano, Preliminary study of the effects of ageing on the long-term performance of NPP pipe, *Prog. Nucl. Energy*, vol. 131, 103573, 2021
- [32] Total Material Database; <https://www.totalmateria.com/>
- [33] IAEA, Material degradation and related managerial issues at nuclear power plants Proceedings of a Technical Meeting, Vienna, 15–18 February 2005. IAEA Proceedings series, 2006
- [34] S. Oh, et al., On-Line Monitoring of Pipe Wall Thinning by a High Temperature Ultrasonic Waveguide System at the Flow Accelerated Corrosion Proof Facility, *Sensors*, vol. 19, n. 8, 2019
- [35] O. K. Chopra, Estimation of Fracture Toughness of Cast Stainless Steels During Thermal Aging in LWR Systems, US NRC, NUREG/CR 4513, 2016
- [36] O. K. Chopra and A. S. Rao, Methodology for Estimating Thermal and Neutron Embrittlement of Cast Austenitic Stainless Steels During Service in Light Water Reactors», *J. Press. Vessel Technol.*, vol. 138, n. 040801, 2016
- [37] O. Obeid, et al., Experimental and numerical thermo-mechanical analysis of welding in a lined pipe, *Journal of Manufacturing Processes*, vol. 32, 857-872, 2018
- [38] MSC Marc Manuals, vol. A, 2020.
- [39] G. A. Zhang, et al., A study of flow accelerated corrosion at elbow of carbon steel pipeline by array electrode and computational fluid dynamics simulation, *Corrosion Science*, vol. 77, 334-341, 2013

